



MDOT RC-1563



## High Skew Link Slab Bridge System with Deck Sliding over Backwall or Backwall Sliding over Abutments

**FINAL REPORT – SEPTEMBER 2011**

Part I



**Western Michigan University**  
Department of Civil & Construction Engineering  
College of Engineering and Applied Sciences

**RESEARCH**

Intentionally left blank

Technical Report Documentation Page

1. Report No. <b>Research Report RC-1563</b>	2. Government Accession No.	3. MDOT Project Manager <b>Steve Kahl, P.E.</b>	
4. Title and Subtitle <b>High skew link slab bridge system with deck sliding over backwall or backwall sliding over abutments</b>		5. Report Date <b>September 30, 2011</b>	
7. Author(s) <b>Dr. Haluk Aktan, P.E., and Dr. Upul Attanayake, P.E.</b>		6. Performing Organization Code <b>WMU</b>	
9. Performing Organization Name and Address <b>Department of Civil and Construction Engineering College of Engineering and Applied Sciences Western Michigan University 1903 W. Michigan Ave, Kalamazoo, MI 49008</b>		8. Performing Org Report No.	
12. Sponsoring Agency Name and Address <b>Michigan Department of Transportation Construction and Technology Division PO Box 30049, Lansing MI 48909</b>		Work Unit No.	
		11. Contract Number : <b>2006-0415</b>	
		11(a). Authorization Number: <b>3</b>	
15. Supplementary Notes		13. Type of Report and Period Covered <b>Final Report, 2008-2011</b>	
		14. Sponsoring Agency Code	
16. Abstract <p>A new bridge design and construction trend to help improve durability and rideability is to remove expansion joints over piers and abutments. One approach to achieve this is to make the deck continuous over the piers by means of a link slab while the girders remain simply supported. The need to implement link slabs is indicated by AASHTO LRFD section 2.5.2.4 which requires using a minimum number of expansion joints to improve rideability. Further, due to durability concerns associated with bridge deck joints, it is preferred to have a least number of joints or develop jointless decks. The expansion joints over the abutments can be removed by one of three methods: deck sliding over back wall, semi-integral abutments, and integral abutments. This results in expansion joints at either or both ends of the approaches. The design concerns other than link slab include backwall and wing-wall design and bearing movement. The behavior of a jointless bridge brings about many challenges to bridge designers. The complexity is augmented when skew is involved.</p> <p>This report complements an earlier report based on previous research on <i>Combining Link Slab, Deck Sliding Over Backwall and Revising Bearings</i> (Aktan et al., 2008) where the behavior of straight and moderately skew (skew &lt; 20<sup>0</sup>) link slab bridges were investigated and design recommendations were developed. This report describes the behavior and performance of high skew (skew &gt; 20<sup>0</sup>) jointless bridges with link slabs and two abutment configurations. These abutment configurations are deck sliding over backwall and backwall sliding over abutments (i.e. semi-integral abutments).</p> <p>Four tasks were performed in this project. The first task was to review and synthesize information related to the behavior, performance, design, and analysis of skew bridges. The second task was field assessment of skew bridge behavior under static truck loads and thermal loads. The third task was analytical and numerical analysis of skew link slabs. The final task was analytical and numerical analysis of skew sliding deck over backwall systems and semi-integral abutments.</p> <p>Design recommendations are developed based on literature, field assessment data analysis, finite element modeling, and subsequent simulations of the numerous models developed in this project. One recommendation deals with the skew link slab design and the remaining recommendations are for bearing selection and selection and design of a transverse restraint system at abutments of skew link slab bridges.</p>			
17. Key Words: <b>Abutment, Concrete, Finite Element, Jointless Bridge, Link Slab, and skew.</b>		18. Distribution Statement <b>No restrictions. This document is available to the public through the Michigan Department of Transportation.</b>	
19. Security Classification (report) <b>Unclassified</b>	20. Security Classification (Page) <b>Unclassified</b>	21. No of Pages <b>249</b>	22. Price

Intentionally left blank

# High Skew Link Slab Bridge System with Deck Sliding over Backwall or Backwall Sliding over Abutments

Project Manager: Mr. Steve Kahl, P.E.

Submitted to:



Submitted by

Dr. Haluk Aktan, P.E.  
Professor & Chair  
(269) – 276 – 3206  
[haluk.aktan@wmich.edu](mailto:haluk.aktan@wmich.edu)

Dr. Upul Attanayake, P.E.  
Assistant Professor  
(269) – 276 – 3217  
[upul.attanayake@wmich.edu](mailto:upul.attanayake@wmich.edu)



**Western Michigan University**  
Department of Civil & Construction Engineering  
College of Engineering and Applied Sciences  
Kalamazoo, MI 49008  
Fax: (269) – 276 – 3211

Intentionally left blank

## **DISCLAIMER**

The content of this report reflects the views of the authors, who are responsible for the facts and accuracy of the information presented herein. This document is disseminated under the sponsorship of the Michigan Department of Transportation in the interest of information exchange. The Michigan Department of Transportation assumes no liability for the content of this report or its use thereof.

Intentionally left blank



## **ACKNOWLEDGEMENTS**

This project is funded by the Michigan Department of Transportation. The authors would like to acknowledge the support and effort of Mr. Steve Kahl for initiating this research. The authors also wish to acknowledge the continuing assistance of the Research Advisory Panel (RAP) members in contributing to the advancement of this study. Contribution of graduate students Abdul Mohammed, Alp Servi, Duy Nguyen, Michael Romkema, and Mohamed Rusthi for the successful completion of this study is highly appreciated.

Intentionally left blank

# **EXECUTIVE SUMMARY**

## **INTRODUCTION**

The new bridge design trend is to avoid having expansion joints over piers and abutments to prevent premature deterioration of bridges due to faulty joints. For this purpose joints over the piers are eliminated using link slabs where the deck is continuous and the underlying girders are simply supported. The expansion joints over the abutments are also eliminated by allowing the deck to slide over the backwall or by allowing the deck-backwall combined system to slide over the abutment (semi-integral abutments). As a result, the movement of the superstructure is transferred to the ends of the approach slab that sits on a sleeper slab.

This research was designed to respond to the concerns of the designers in terms of the design of specific components of high skew jointless link slab bridges with deck sliding over backwall or semi-integral abutment configurations.

The objectives of this study were identified as follows:

1. Study the behavior of high skew bridge structural system by load testing and analytical modeling and analysis.
2. Develop finite element models of selected components, or combinations of several components, of the link slab bridge deck system with deck sliding over backwall and semi-integral abutment to understand the behavior and interaction between components under various load conditions, including volume change load.
3. Develop recommendations for changes or modifications to the design of the link slab, and bearings, abutment types, and lateral restraint systems of bridges with link slabs.

To satisfy the objectives, this project was organized into four main tasks: literature review, field assessment of skew bridge behavior under static truck loads and thermal loads, analytical and numerical analysis of skew link slabs, and analytical and numerical analysis of skew sliding deck over backwall systems and semi-integral abutments.

## LITERATURE REVIEW

Literature on the following topics was reviewed: skewed bridge behavior under gravity loading, skewed bridge behavior under volume change loads, design challenges of skewed/jointless bridges, and performance of skew/ jointless bridges. A summary of key points identified through literature review is given below:

1. Skewed bridges with semi-integral abutments would tend to rotate about an axis normal to their horizontal plane. The rotation is due to the passive pressure developed behind the backwall under thermal expansion. Deck extensions also have a tendency to develop in-plane rotations but not as critical as semi-integral systems. In both deck extension and semi-integral systems, the rotation may be affected by the approach slab-base interface friction, the shearing resistance of the elastomers in the bearings, and by the compressive resistance of fillers used in the movable joints between the superstructure and wingwalls.
2. The current MDOT deck sliding over backwall system uses Expanded polystyrene (EPS) in between deck and backwall to introduce the sliding surface. The EPS elastic strain limit is very small and can deform beyond the elastic limit under deck self-weight and live loads. Further, peak and residual friction coefficients between EPS and concrete are 2.3 and 1.0, respectively. Because of these reasons, neoprene pads over backwall may be used. In addition, the polyethylene sheet used under approach should be extended to the backwall face on the span side to minimize friction at the interface.
3. A current semi-integral configuration used by Ontario and several State Highway Agencies has the advantages of allowing the backwall to move independently from the abutment, providing access space for bearing inspection, maintenance, and replacement; and preventing backfill infiltration through the backwall.
4. Isolation of the backwall from its abutment requires developing specific design details to constrain transverse movement of skew bridges. In that regard, placing the backwall over the abutment and restraining transverse movement by placing the

- wingwall against the backwall and deck, similar to the current MDOT semi-integral details, provides many benefits if adequate measures are taken to minimize interface friction and infiltration of backfill material through the joints. Use of EPS form behind the backwall helps reduce passive earth pressure and prevent infiltration of backfill material.
5. In order to allow the translation and rotation of skew bridges and provide sufficient load capacity, plain elastomeric pad (PEP), fiberglass-reinforced pad (FRP), and steel-reinforced elastomeric bearings or pads (SREB or SREP) are suitable for support bearings for semi-integral and deck sliding over backwall bridges. Also, polytetrafluorethylene (PTFE) sliding bearings can be combined with the support bearing types stated above to accommodate large superstructure movements.
  6. Rub plates, girder stops, or any other mechanism designed to resist large forces is needed to control lateral movement of skew bridges.
  7. With increasing backfill stiffness, forces at the wingwalls of high skew bridges increase dramatically. EPS can be specified as a suitable backfill material for semi-integral bridges to reduce passive pressure. However, an approach slab should not be directly supported on EPS because of potential creep. EPS should also be protected using geotextiles and gasoline containment geomembranes.

#### **FIELD ASSESSMENT OF SKEW BRIDGE BEHAVIOR UNDER STATIC TRUCK LOADS AND THERMAL EXPANSION**

Bridge deflections and bearing translations were measured under static truck as well as thermal loads. Measured girder deflections showed that girder end movements were controlled by bearing friction. It is worth mentioning here that the bearing movements under static truck loads were very small compared to allowance made at the design for thermal expansion and contraction. The measured bearing movement under thermal expansion loads from May to July indicates that the bearings are frozen and an in-plane twist of the deck occurs due to bearing movement that is not expected at the design stage. Though there was no damage to the superstructure and substructure of this 120 ft long single span bridge, this

behavior is critical when link slabs are implemented and the deck over the abutments is made continuous. The observations highlight the importance of using durable bearings that are capable of accommodating large deformation and a certain degree of rotation demands.

## **LINK SLAB ANALYSIS FOR DEVELOPING DESIGN GUIDELINES**

Finite element analysis was utilized to understand the behavior of the jointless skew bridge structural system with link slabs to verify the design assumptions and propose fine-tuning to the current link slab design procedures to accommodate changing load demands due to bridge skew. This task was accomplished by developing and analyzing refined finite element models representing a two span bridge with a skew link slab. The major interest is how skew affects the link slab moments. Skew reduction factors were calculated using moment ratios and presented in Chapter 4. Skew reduction factors vary significantly with the live load configurations, support configurations under the link slab, and with the direction of moment (i.e., negative or positive). Skew reduction factors show that load demand decreases with increasing skew.

A detailed link slab design example is given in Appendix C. The 45<sup>0</sup> skew bridge, in this case, has a RHHR (Roller-Hinge-Hinge-Roller) support configuration, which develops the largest link slab moments and forces under applied loads. Yet, the amount of required link slab reinforcement is governed by the minimum reinforcement amount requirements of AASHTO LRFD (2010).

Following are further key summary observations on analysis results:

1. The RHHR boundary condition develops significantly larger link-slab moments compared to other support conditions.
2. NTG can be excluded from design load combination with HRRR and RRHR support conditions.
3. NTG load case moments that develop in the link slab of bridges with zero skew and RHHR support configuration, should be directly used in design without any reduction for skew.
4. The negative moment design of a link slab with the RHHR support configuration is governed by the combined effect of live and NTG loads.

5. Positive moment design of a link slab with the RHHR support configuration is governed by a PTG load.
6. Moment developed in a link slab under thermal gradient loads (PTG and NTG) remains constant irrespective of span.
7. Providing the minimum reinforcement amount required in AASHTO LRFD Section 5.7.3.3.2 is adequate for the majority of skew link slabs with HRRR or RRHR support configuration for spans up to 110 feet. However, additional reinforcement at the bottom layer is needed to resist large tensile stresses developed near the boundaries of the debonded region. A top layer of #6 bars at 4 in. spacing and bottom layer of #6 bars at 4 in. spacing are adequate for high skew link slabs. Proposed detail in standard MDOT Bridge Design Guide format is presented in Appendix E.
8. Simplified analysis models are not able to represent three dimensional effects such as positive moments under live load or negative moments under PTG. New analysis models and procedures are required.

## **SKEW ABUTMENT ANALYSIS AND DESIGN GUIDELINES**

This report provides a detailed analysis of two skew abutment configurations namely deck sliding over backwall and semi-integral systems for a range of skew angles from  $0^{\circ}$  to  $45^{\circ}$  under loads and configurations specified in AASHTO (2010) and Michigan Bridge Design Manual (MDOT 2005). Deck sliding over backwall and semi-integral abutment details presented in Aktan et al. (2008) represented the basis of the FE models. These models were modified to incorporate various bearing configurations and wingwalls. The following is a summary of conclusions that are derived based on analysis results and information presented in related literature and design specifications /guidelines

1. A bridge span with deck sliding over backwall or semi-integral abutments can be analyzed as simply supported spans to calculate girder end rotations and translation (expansion/contraction) demands.
2. Skew bridges expand and contract along the diagonal between acute corners. The movement results in transverse forces at the bearings and other restraint systems. The restraint force magnitudes become considerably larger if adequate tolerances are not

provided to accommodate the movements due to thermal loads. The situation requires special consideration when link slabs are implemented over the piers, which in turn increase the effective length of thermal expansion and contraction. Further, the direction of bridge movement under expansion and contraction loads needs to be restricted to the bridge axis. In plane twisting results in large stresses along the edge of link slab (see Chapter 4). Link slab is also flexible under torsion compared to the deck-girder integrated system. Hence, controlling bridge alignment is critical when link slabs are implemented.

3. It is recommended that deck sliding over backwall abutments, is restrain the transverse movement of the center girder end (for odd number of girders) or two centermost girder ends (for even number of girders) using concrete keys with rub plates (shown on Figure 5-8.). Also, larger tolerance is required for the slot in the sole plate and bearings in order to accommodate the transverse movement of unrestrained girder ends. Proposed detail in standard MDOT Bridge Design Guide format is presented in Appendix F. The required formulations and variables for movement calculations are presented with the drawings. The rub plate design procedure is based on the VDOT Bridge Design Manual section 20.04 (2010) with modifications and presented in Appendix G.
4. Transverse movement of bearings over the semi-integral abutment is facilitated by increasing the tolerance of the slot at the bearing plate. Transverse restraint for expansion thermal load is provided by a wingwall at the acute corner. Alignment of semi-integral abutment bridge deck with backwall offset from the abutment is managed under contraction thermal loads by placing a concrete key at the center girder. Calculation of the transverse force on the wingwall is adopted from the procedure described in VDOT (2010). Proposed detail in standard MDOT Bridge Design Guide format is presented in Appendix H.
5. It is recommended that an EPS layer is placed behind the backwall of semi-integral bridges. This will minimize the passive pressure and results in lower transverse forces at the wingwall. Although the passive pressure coefficient of EPS is in reality



much lower than four (4), a coefficient of four (4) is recommended for conservative design until additional supporting data is developed (VDOT (2010)). Further, the equation given in VDOT (2010) section 20-06-6 can be used to calculate EPS layer thickness (i.e., Eq. 2-2 in Chapter 2 section 2.4.4).

6. It is recommended that the maximum bearing tolerance in transverse direction is limited to 0.25 in. Further investigations can be carried out analyzing the impact of the increased fit tolerances of the girder position dowels on the bridge components.
7. Following link slabs are implemented, controlling friction at the approach slab interfaces is very critical. Increased friction hinders bridge movement restricting expansion bearing movement over the abutment. This results in stresses greater than the concrete modulus of rupture under negative thermal loads. Hence, it is vital to reduce friction at all the contract surfaces at the abutment and approach to facilitate movement of the bridge under expansion and contraction thermal loads. To reduce friction a 0.025 in. thick polyethylene sheet can be placed during construction over the fill supporting the approach slab.
8. Bridge expansion length, which is the distance along the longitudinal axis measured from abutment to the nearest fixed bearing, is a function of bridge length, width, and skew. Expansion joint effective movement rating and allowable movement at bearings are the limiting factors of bridge expansion length when link slabs are implemented. Hence, the bridge expansion length should be calculated following the procedure given in chapter 5 and be enforced when link slabs are implemented. As an example, based on maximum strip seal joint width of 3 in. and expansion and contraction thermal load of 115 °F, the following maximum expansion length are recommended:

Straight concrete bridge  $\leq$  300 ft.

45° skew concrete bridge of 100 ft wide  $\leq$  200 ft.

Straight steel bridge  $\leq$  275 ft.

45° skew steel bridge of 100 ft wide  $\leq$  175 ft.

## CONCLUSIONS

A literature review was performed, along with a field assessment of a skew bridge behavior under static truck loads and thermal loads, an analytical and numerical analysis of skew link slabs, and an analytical and numerical analysis of skew sliding deck over backwall systems and semi-integral abutments tasks.

Current link slab design procedures do not incorporate skew effects. A design procedure was developed following a detailed analysis of skew link slabs and the moment and force envelopes for various boundary and load configurations. Two major findings are (1) moment developed in a link slab under temperature gradient loads remains constant irrespective of span and (2) moment developed in a link slab under live load decreases with increased span. Analysis results verified that the minimum reinforcement amount required in AASHTO LRFD Section 5.7.3.3.2 is adequate for the majority of skew link slabs with HRRR or RRHR support configuration. However, additional reinforcement at the bottom layer is needed to resist large tensile stresses that develop near the boundaries of the debonded region. A detailed design example is presented in Appendix C. Proposed link-slab detail in standard MDOT Bridge Design Guide format is presented in Appendix E. Three saw cuts are recommended: one at each end of the link slab and one directly over the pier centerline.

The implementation of link slabs on deck sliding over backwall and semi-integral systems presents specific challenges. This report provides a detailed analysis of two skew abutment configurations namely deck sliding over backwall and semi-integral systems for a range of skew angles from  $0^{\circ}$  to  $45^{\circ}$  under loads and configurations specified in AASHTO (2010) and Michigan Bridge Design Manual (MDOT 2005). Bearing details, wingwall and concrete key configurations, and abutment configurations were developed. Proposed detail in standard MDOT Bridge Design Guide format is presented in Appendix F and H. All the required mathematical relationships and variables are presented with the drawings. The rub plate design procedure was adopted from VDOT Bridge Design Manual section 20.04 (2010) with some modifications and presented in Appendix G.

## TABLE OF CONTENTS

<b>ACKNOWLEDGEMENTS .....</b>	<b>ix</b>
<b>EXECUTIVE SUMMARY .....</b>	<b>xi</b>
<b>LIST OF TABLES.....</b>	<b>xxiii</b>
<b>LIST OF FIGURES .....</b>	<b>xxv</b>
<b>1 INTRODUCTION .....</b>	<b>1</b>
1.1 Overview.....	1
1.2 Project Objectives and Tasks.....	2
1.3 Report Organization.....	2
<b>2 STATE-OF-THE-ART LITERATURE REVIEW .....</b>	<b>5</b>
2.1 Overview.....	5
2.2 Skewed Bridge Behavior under Gravity Loading.....	7
2.2.1 Finite Element (FE) Simulation of Skew Bridge Behavior under Gravity Loading.....	9
2.3 Skewed Bridge Behavior under Volume Change Loads .....	16
2.3.1 Skew Bridge Behavior under Thermal Loads.....	21
2.4 Design Challenges of Skewed/Jointless Bridges .....	34
2.4.1 Length, Skew and Curvature Limits .....	34
2.4.2 Volume Change Loads and Behavior of Jointless Bridges.....	35
2.4.3 Semi-Integral Abutment Details .....	39
2.4.4 EPS Backfill.....	45
2.4.5 EPS-Concrete Interface Friction.....	49
2.4.6 Support Bearing Selection and Design .....	49
2.4.7 Deck Reinforcement Details with Skew .....	54
2.5 Field Performance of Skewed/Jointless Bridges.....	56
2.6 Summary .....	60
<b>3 MODELING AND FIELD TESTING OF A HIGH SKEW BRIDGE ..</b>	<b>63</b>
3.1 Objective and Approach .....	63
3.2 Bridge Description.....	63

3.3	Abutment, Bearing, and Deck Condition.....	69
3.3.1	Abutment Condition.....	69
3.3.2	Bearing Condition.....	69
3.3.3	Deck Condition .....	72
3.4	FE Modeling and Preliminary Analysis for Load Testing.....	73
3.4.1	Bridge FE Modeling .....	73
3.4.2	Truck Placement and Loading Configurations .....	74
3.4.3	Calculated Bridge Deflections and Translations.....	75
3.5	Measured Bridge Deflections and Translations.....	78
3.5.1	Field Measurement Equipment and Procedures .....	78
3.5.2	Bridge Deflection.....	86
3.5.3	Bearing Translation.....	90
3.6	Summary .....	98
<b>4</b>	<b>LINK SLAB ANALYSIS AND DESIGN GUIDELINES .....</b>	<b>99</b>
4.1	Overview and Objectives.....	99
4.2	Contact Simulation.....	99
4.3	Modeling and Analysis of a Link Slab Bridge.....	101
4.3.1	Overview and Objectives.....	101
4.3.2	Prototype Bridge .....	101
4.3.3	Material Properties.....	102
4.3.4	Bridge Model Geometry .....	102
4.3.5	Bridge Model Orientation .....	104
4.3.6	Link Slab Length.....	105
4.3.7	FE Discretization of the Bridge Model.....	105
4.3.8	Skew Mesh.....	106
4.3.9	Contact Surfaces in the FE Model .....	109
4.3.10	Boundary Conditions .....	110
4.3.11	Loads.....	110
4.4	Sign Convention, Model Verification, and Results .....	114
4.4.1	Overview.....	114
4.4.2	Sign Convention.....	114

4.4.3	FE Model Verification .....	115
4.4.4	Results.....	116
4.4.5	Skew Link Slab Design Procedure .....	163
<b>5</b>	<b>SKEW ABUTMENT ANALYSIS AND DESIGN GUIDELINES .....</b>	<b>169</b>
5.1	Overview and Objectives.....	169
5.2	Abutment Configurations and Analysis Models.....	169
5.3	Lateral Restraint Systems in Skew bridges.....	173
5.3.1	Restraint Systems at the Abutment .....	175
5.3.2	Restraint System over the Pier .....	175
5.4	Analysis of High Skew Bridge with Deck Sliding over Backwall and Semi-Integral Abutments .....	175
5.4.1	Material Properties.....	176
5.4.2	Loads.....	176
5.4.3	Load Combinations.....	182
5.4.4	Boundary Conditions .....	183
5.4.5	Deck Sliding over Backwall Abutment .....	184
5.4.6	Semi-Integral Abutment.....	199
5.5	Analysis and Design Procedures and Details for Abutments and Bearings .....	205
<b>6</b>	<b>SUMMARY, CONCLUSIONS, DESIGN RECOMMENDATIONS, AND IMPLEMENTATION PLAN .....</b>	<b>209</b>
6.1	Summary and Conclusions .....	209
6.2	Recommendations.....	210
6.2.1	Link Slab Design.....	210
6.2.2	Deck Sliding over Backwall .....	211
6.2.3	Semi-Integral Abutment.....	211
6.3	Implementation Plan .....	212
<b>7</b>	<b>REFERENCES .....</b>	<b>213</b>
<b>APPENDIX A: Acronyms and Abbreviations</b>		
<b>APPENDIX B: Holland Bridge Data</b>		
<b>APPENDIX C: High Skew Link Slab Design - Example</b>		
<b>APPENDIX D: Link Slab Moment due to Thermal Gradient (MathCAD)</b>		

**APPENDIX E:** Proposed Details for Skew Link Slab

**APPENDIX F:** Proposed Details for Deck Sliding over Backwall System

**APPENDIX G:** Rub Plate Design Procedure

**APPENDIX H:** Proposed Details for Semi-Integral Abutments

## LIST OF TABLES

Table 2-1. Range of Design Criteria Used for Selection of Jointless Bridges.....	34
Table 2-2. Bearing Suitability (Source: AASHTO LRFD 2010) .....	50
Table 2-3. Summary of Bearing Capabilities (Source: Roeder and Stanton 1996).....	50
Table 3-1. Bridge Components, Dimensions, and Element Types used in the Model .....	73
Table 3-2. Ambient Conditions at 2:30pm on December 16 2010.....	85
Table 3-3. Target Position Coordinates – Baseline Measurements (Dec. 16, 2010).....	86
Table 3-4. Girder-End Translations over South Abutment under Uniform Temperature Loading .....	97
Table 4-1. ABAQUS Syntax for Various Contact Options .....	100
Table 4-2. Bearing Configurations and Corresponding Support Conditions.....	110
Table 4-3. Total Sectional Moment and Force Variation Trend with Increased Skew under Various Load and Support Configurations .....	131
Table 4-4. Skew Reduction Factors for HRRR .....	159
Table 4-5. Skew Reduction Factors for RRHR .....	160
Table 4-6. Skew Reduction Factors for RHHR .....	161
Table 4-7. Girder-End Rotations and Skew Reduction Factors - Lane1 Load Case .....	162
Table 4-8. Girder-End Rotations and Skew Reduction Factors - Lane2 Load Case .....	162
Table 4-9. Girder-End Rotations and Skew Reduction Factors – LaneAlt1 Load Case.....	162
Table 4-10. Girder-End Rotations and Skew Reduction Factors – LaneAlt2 Load Case....	162
Table 4-11. Girder-End Rotations and Skew Reduction Factors - NTG Load Case .....	162
Table 4-12. Girder-End Rotations and Skew Reduction Factors - PTG Load Case.....	163
Table 4-13. Material and Geometric Properties used in Link Slab Design Example .....	164
Table 4-14. Analytical Rotation and Analytical Design Moment Magnitudes .....	165
Table 4-15. Ratios of 3D FE to Analytical Design Moment for a Straight Bridge .....	165
Table 4-16. Analytical Rotation and Analytical Design Moment Magnitudes for Different Spans .....	166
Table 4-17. Ratio of 3D FE to Analytical Bending Moment for Straight Bridge with Different Spans .....	167
Table 5-1. Girder End Rotations against Different Truck Positions on Skew Bridge.....	181

Table 5-2. Thermal Load for Bridge Expansion and Contraction ..... 182  
Table 5-3. Expansion and Contraction of Girder 1 End over Semi-Integral Abutment ..... 201



## LIST OF FIGURES

Figure 2-1. Geometric relation of skew angle and angle of crossing .....	6
Figure 2-2. Percentages of skew bridges in Michigan.....	6
Figure 2-3. Percentage of skewed bridges in Michigan (a) concrete and (b) steel.....	7
Figure 2-4. Load distribution pattern in skewed stringer and slab bridges.....	8
Figure 2-5. Characteristics of skewed slab deck (Hambly 1991). .....	8
Figure 2-6. (a) Cross section and (b) isometric views of the stringer models .....	10
Figure 2-7. Plan view of FE models .....	10
Figure 2-8. Transverse bending stress distribution of deck for (a) stringer bridge deck and (b) solid slab for 40° skew under self-weight .....	12
Figure 2-9. Longitudinal bending stress distribution (a) stringer (b) solid slab bridge of 40° skew under self-weight (negative moment regions only) .....	12
Figure 2-10. Longitudinal bending moment variation against skew for full-width stringer bridge under self-weight .....	13
Figure 2-11. Longitudinal bending moment variation against skew for full-width stringer bridge under a concentrated load .....	13
Figure 2-12. Mid-span moment variation vs. skew angle under self-weight and concentrated load for stringer bridge.....	14
Figure 2-13. Torsion for full-width of stringer bridge under self-weight.....	14
Figure 2-14. Torsion for full-width of stringer bridge under concentrated load .....	15
Figure 2-15. Support reaction vs. skew angle for stringer bridge under self-weight.....	15
Figure 2-16. Direction of skew simply supported bridge movement under uniform thermal load.....	16
Figure 2-17. Bearing orientation for constraint cases (a) traditional, (b) radial from corner, (c) radial from center (Tindal and Yoo 2003).....	17
Figure 2-18. Longitudinal displacement profile of deck for right and 45° skew bridge.....	19
Figure 2-19. Transverse displacement profile of deck for right and 45° skew bridge.....	20
Figure 2-20. Maximum normalized longitudinal and transverse displacement vs. skew angle .....	20
Figure 2-21. Forces on deck due to resistance encountered in expansion joints .....	21

Figure 2-22. Positive and negative temperature gradient loads used in the analyses .....	22
Figure 2-23. Displacement contours under the traditional bearing condition for skew angles .....	23
Figure 2-24. Displacement contours under radial from corner bearing condition for skew angles .....	24
Figure 2-25. Displacement contours under the radial from center bearing condition for skew angles .....	25
Figure 2-26. Deformed shape under the traditional bearing condition for skew angles.....	26
Figure 2-27. Deformed shape under radial from corner bearing condition for skew angles .	27
Figure 2-28. Deformed shape under radial from center bearing condition for skew angles .	28
Figure 2-29. Transverse (left) and longitudinal (right) displacement contours under the traditional bearing condition for skew angles (a) 0° (b) 15° (c) 30° (d) 45° (e) 60° .....	30
Figure 2-30. Transverse (left) and longitudinal (right) displacement under the radial from corner bearing condition for skew angles (a) 0° (b) 15° (c) 30° (d) 45° (e) 60° .....	31
Figure 2-31. Transverse (left) and longitudinal (right) displacement under the radial from center bearing condition for skew angles (a) 0° (b) 15° (c) 30° (d) 45° (e) 60° .....	32
Figure 2-32. Longitudinal bending moment for full-width of simply supported stringer bridge under negative temperature gradient .....	33
Figure 2-33. Torsion for full-width of simply supported stringer bridge under negative temperature gradient .....	33
Figure 2-34. Percent of states that account for different forces in the design of jointless bridges.....	35
Figure 2-35. Resultant force components that develop at the abutment under thermal expansion (Oesterle et al. 1999).....	36
Figure 2-36. Forces on the bridge (Steinberg et al. 2004) .....	37
Figure 2-37. Deformed shape of the deck of a two-span continuous skew stringer bridge under uniform expansion .....	38
Figure 2-38. Rub plate detail (VDOT).....	39

Figure 2-39. VDOT deck extension detail with buried approach slab .....	40
Figure 2-40. Semi-integral abutment detail with end diaphragm moving over a fixed abutment.....	41
Figure 2-41. Semi-integral abutment details of concrete girder bridge with overall span < 328 ft .....	42
Figure 2-42. Semi-integral abutment details of concrete girder bridge with overall span > 328 ft .....	43
Figure 2-43. Semi-integral abutment details of steel girder bridge with overall span < 328 ft .....	44
Figure 2-44. Semi-integral abutment details of steel girder bridge with overall span > 328 ft .....	44
Figure 2-45. VDOT semi-integral system with EPS (Hoppe 2005) .....	46
Figure 2-46. Typical details of EPS abutment (Stark et al. 2004) .....	48
Figure 2-47. Deck sliding over backwall: (a) NYDOT and (b) MDOT .....	49
Figure 2-48. Preliminary bearing selection diagram for minimal design rotation (rotation $\leq$ 0.005 radians) (source: Roeder and Stanton 1996).....	51
Figure 2-49. Preliminary bearing selection diagram for moderate design rotation (rotation $\leq$ 0.015 radians) (source: Roeder and Stanton 1996).....	51
Figure 2-50. Preliminary bearing selection diagram for large design rotation (rotation > 0.015 radians) (source: Roeder and Stanton 1996).....	52
Figure 2-51. Preliminary bearing selection diagram (Badie, et al. 2001).....	52
Figure 2-52. MDOT semi-integral abutment configuration .....	53
Figure 2-53. Backwall and abutment configuration of a bridge with different girder depths	54
Figure 2-54. Reinforcement layout (AASHTO LRFD 2007).....	54
Figure 2-55. End zone reinforcement details (MDOT Bridge Design Guide 6.41.02) .....	56
Figure 2-56. Link slab cracking on S08 of 63101 (Gilani and Jansson 2004).....	57
Figure 2-57. Link slab design detail and an inspection photo (Gilani and Jansson 2004) ....	58
Figure 2-58. Abutment wall cracking near an acute corner of the superstructure .....	59
Figure 2-59. Semi-integral abutment configuration used by the Ontario MOT before most recent details .....	60
Figure 3-1. Bridge location (Source: Google map) .....	64

Figure 3-2. Arial view of the bridge (Source: Google map).....	64
Figure 3-3. Isometric and elevation views of the bridge .....	65
Figure 3-4. Schematic view of bridge cross section .....	65
Figure 3-5. Schematic view of diaphragms and girders with labels .....	66
Figure 3-6. Schematic view of end and intermediate diaphragms (cross frames) .....	66
Figure 3-7. Schematic view of abutment section with backwall, girder and foundation.....	67
Figure 3-8. Schematic view of girder plan and elevation .....	68
Figure 3-9. Schematic view of respective bearing details .....	69
Figure 3-10. Interior and exterior bearing condition at north abutment .....	70
Figure 3-11. Expansion bearing and joint condition at south abutment .....	70
Figure 3-12. Expansion bearing condition at south abutment .....	71
Figure 3-13. Expansion joint and deck condition .....	72
Figure 3-14. FE model configuration.....	73
Figure 3-15. Truck configuration and wheel loads .....	74
Figure 3-16. Truck positions and bridge configuration .....	75
Figure 3-17. Mutually exclusive bridge loading configurations.....	75
Figure 3-18. Girder labels and 16 displacement measurement points .....	76
Figure 3-19. Girder bottom flange out of plane deformation, girder end translations, and vertical deflection contours under loading configuration-I .....	76
Figure 3-20. Girder bottom flange out of plane deformation, girder end translations, and vertical deflection contours under loading configuration-II .....	77
Figure 3-21. Girder bottom flange out of plane deformation, girder end translations, and vertical deflection contours under loading configuration-III.....	77
Figure 3-22. Girder bottom flange out of plane deformation, girder end translations, and vertical deflection contours under loading configuration-IV.....	78
Figure 3-23. Laser Tracker .....	79
Figure 3-24. Reflectors (targets) used with the Laser Tracker .....	80
Figure 3-25. AT MeteoStation.....	80
Figure 3-26. Graphical user interface (GUI) window.....	80
Figure 3-27. Accessories used for mounting girder end and abutment targets.....	82
Figure 3-28. Laser Tracker, server, and computer.....	83

Figure 3-29. South abutment of the westbound bridge (targets on abutment and girder ends)	84
Figure 3-30. North abutment of the westbound bridge (targets on abutment and girder ends)	84
Figure 3-31. Target positions on girders	85
Figure 3-32. Coordinate system for Tracker measurements and target positions on north abutment and girder ends	85
Figure 3-33. Truck configurations and wheel loads	87
Figure 3-34. Truck positions and bridge configuration	87
Figure 3-35. Mutually exclusive bridge loading configurations	88
Figure 3-36. Girder A deflection under loading configuration II	89
Figure 3-37. Girder G deflection under loading configuration IV	89
Figure 3-38. Bearing movement under truck loads (FE analysis)	90
Figure 3-39. 3-D view of bearing movement (towards south abutment) under loading configuration IV	91
Figure 3-40. Bearing movement under truck loads (Tracker measurements)	92
Figure 3-41. Bearing positions after loading and unloading following load configuration II and IV	92
Figure 3-42. Bearing translation under uniform thermal loads (FE analysis)	94
Figure 3-43. Maximum and minimum daily temperature variation at the site	95
Figure 3-44. Average temperature variation at the site	96
Figure 3-45. Bearing translation from Dec. 2010 to May 2011 and July 2011 (Tracker measurements)	97
Figure 4-1. Cross section of Bridge S12-7 of 25042	101
Figure 4-2. Current MDOT requirements for two-lane highway bridges	102
Figure 4-3. MDOT New Jersey Type 4 barriers	103
Figure 4-4. Cross section of bridge	103
Figure 4-5. Elevation view of FE bridge	104
Figure 4-6. Bridge model orientation and labeling system	104
Figure 4-7. Cross section view of single girder and deck	106
Figure 4-8. Elevation view of mesh at link slab region	106

Figure 4-9. Isometric view of bridge models.....	107
Figure 4-10. Skew link slab mesh.....	108
Figure 4-11. Contact surfaces in the FE models.....	109
Figure 4-12. Abaqus syntax used in FE bridge model.....	109
Figure 4-13. Bearing configuration layout.....	110
Figure 4-14. Live load cases.....	111
Figure 4-15. Truck and lane load locations.....	112
Figure 4-16. Temperature gradient.....	113
Figure 4-17. Sign convention.....	115
Figure 4-18. Total sectional moment - Lane1 load case.....	118
Figure 4-19. Total sectional moment - Lane2 load case.....	119
Figure 4-20. Total sectional moment – LaneAlt1 load case.....	120
Figure 4-21. Total sectional moment – LaneAlt2 load case.....	121
Figure 4-22. Total sectional moment - NTG load case.....	122
Figure 4-23. Total sectional moment - PTG load case.....	123
Figure 4-24. Total sectional force - Lane1 load case.....	124
Figure 4-25. Total sectional force - Lane2 load case.....	125
Figure 4-26. Total sectional force – LaneAlt1 load case.....	126
Figure 4-27. Total sectional force – LaneAlt2 load case.....	127
Figure 4-28. Total sectional force - NTG load case.....	128
Figure 4-29. Total sectional force - PTG load case.....	129
Figure 4-30. Effective width segments.....	132
Figure 4-31. Effective moment - Lane1 load case.....	133
Figure 4-32. Effective moment - Lane2 load case.....	134
Figure 4-33. Effective moment – LaneAlt1 load case.....	135
Figure 4-34. Effective moment – LaneAlt2 load case.....	136
Figure 4-35. Effective moment - NTG load case.....	137
Figure 4-36. Effective moment - PTG load case.....	138
Figure 4-37. Effective force - Lane1 load case.....	139
Figure 4-38. Effective force - Lane2 load case.....	140
Figure 4-39. Effective Force – LaneAlt1 load case.....	141

Figure 4-40. Effective Force – LaneAlt2 load case .....	142
Figure 4-41. Effective force - NTG load case.....	143
Figure 4-42. Effective force - PTG load case .....	144
Figure 4-43. Edge stresses of link slab with HRRR support conditions under live loads ...	147
Figure 4-44. Edge stresses of link slab with RRHR support conditions under live loads ...	148
Figure 4-45. Edge stresses of a 45 <sup>0</sup> skew link slab under PTG .....	149
Figure 4-46. Stresses developed in 45 <sup>0</sup> skew link slab with HRRR support conditions under LaneAlt1 load case.....	151
Figure 4-47. Gross section moment with and without soft material – LaneAlt1 load case.	152
Figure 4-48. Edge stresses developed under PTG - 45 <sup>0</sup> skew link slab with soft material over girder ends.....	154
Figure 4-49. Link slab bottom fiber stresses under PTG load .....	155
Figure 4-50. Longitudinal stress distribution across north end of the 45 <sup>0</sup> skew link slab bottom fiber under PTG with HRRR support configuration .....	156
Figure 4-51. Longitudinal stress distribution across south end of the 45 <sup>0</sup> skew link slab bottom fiber under PTG with RRHR support configuration .....	156
Figure 4-52. Stresses in link slab with HRRR under PTG .....	157
Figure 4-53. AASHTO Type III girder and composite section geometric properties .....	164
Figure 5-1. Deck sliding over backwall details .....	170
Figure 5-2. Semi-integral abutment details.....	171
Figure 5-3. Semi-integral abutment detail used in Ontario and several other states .....	172
Figure 5-4. Rub plates at backwall - wingwall interface (Source: VDOT 2010) .....	173
Figure 5-5. Rub plates at deck-wingwall interface (Source: VDOT 2010) .....	173
Figure 5-6. Bearing retainer detail (Source: Steinberg and Sargand 2010; Roeder and Stanton 1996) .....	174
Figure 5-7. Dowel bar details for resisting lateral loads on shallow bearing (Source: Roeder and Stanton 1996). .....	174
Figure 5-8. Concrete key system for resisting lateral forces (Source: Roeder and Stanton 1996). .....	174
Figure 5-9. Live load configuration for <i>CASE IV Contraction</i> .....	177
Figure 5-10. Live load configuration for <i>CASE IV Expansion</i> .....	178

Figure 5-11. Location of girder 1 and 8 where girder end rotation was calculated.....	179
Figure 5-12. Truck position 1 for girder end rotation calculation .....	180
Figure 5-13. Truck position 2 for girder end rotation calculation .....	180
Figure 5-14. Truck position 3 for girder end rotation calculation .....	181
Figure 5-15. Deck sliding over backwall model description .....	184
Figure 5-16. Abutment and girder end distress.....	186
Figure 5-17. Girder 1 and 8 end rotation over abutment .....	187
Figure 5-18. Thermal expansion of a skew bridge .....	190
Figure 5-19. Maximum longitudinal bridge contraction and expansion.....	190
Figure 5-20. Variation of concrete bridge expansion length against width and skew when strip seal joint width of 3 in. available for thermal movement .....	191
Figure 5-21. Variation of steel girder bridge expansion against width and skew when strip seal joint width of 3 in. available for thermal movement .....	191
Figure 5-22. Girder 1 and 8 reaction variation over the abutment and pier.....	193
Figure 5-23. Transverse bearing force over abutment under thermal contraction strength load combination.....	196
Figure 5-24. Transverse bearing force over abutment under thermal expansion strength load combination.....	197
Figure 5-25. Typical bearing details .....	198
Figure 5-26. Semi-integral bridge model with wingwalls (not drawn to scale) .....	199
Figure 5-27. Girder 1 reaction of semi-integral bridge .....	200
Figure 5-28. Transverse bearing force over abutment under thermal contraction strength load combination.....	203
Figure 5-29. Transverse bearing force over abutment under thermal expansion strength load combination.....	204
Figure 5-30. Wingwall force due to thermal expansion without transverse restraint over the abutment under strength load combination.....	204



# 1 INTRODUCTION

## 1.1 OVERVIEW

High skew link slab design and design details are described in this report. Abutment and bearing redesign is also described for implementing link slabs on existing high skew bridges during repair activities.

A new bridge design and construction trend to help improve durability and rideability is to remove expansion joints over piers and abutments. One approach to achieve this is to make the deck continuous over the piers by means of a link slab while the girders remain simply supported. The need to implement link slabs is indicated by AASHTO LRFD (2010) section 2.5.2.4 that stipulates the use of minimum number of expansion joints to improve rideability. Further, due to durability concerns associated with bridge deck joints, as stated in Aktan et al. (2002), it is preferred to have as few joints as possible or to develop jointless decks.

In most unremarkable bridges, expansion joints over the abutments can be removed during repair activities. The deck and approach slab can be made continuous based on one of three designs: deck sliding over backwall, semi-integral abutments, and integral abutments. These designs will develop expansion joints at either or both ends of the approaches. Link slabs can be incorporated in repair activities such as partial deck replacement and shallow or deep overlay projects. In the case of full deck replacement, bearings can also be redesigned to allow for the desired movement. The design concerns, other than link slab, include backwall, wing-wall, and bearings. The behavior of jointless bridges brings about many challenges to bridge designers. The complexity is augmented when skew is involved.

The skew policy described in section 7.01.14 of the MDOT Bridge Design Manual (2005), requires special design by refined analysis methods for bridges with skew greater than  $30^{\circ}$  but less than or equal to  $45^{\circ}$ . Further, for skew greater than  $45^{\circ}$ , special approval through bridge design is required. These requirements reflect the complexity of the structure when the skew is involved.

This report complements an earlier report on *Combining Link Slab, Deck Sliding Over Backwall and Revising Bearings* (Aktan et al. 2008) where the behavior of straight and moderately skew ( $\text{skew} \leq 20^\circ$ ) link slab bridges were investigated, and design recommendations were developed. This report will describe the behavior and performance of high skew ( $\text{skew} > 20^\circ$ ) jointless bridges with link slabs and two abutment configurations. These abutment configurations are deck sliding over backwall and backwall sliding over abutments (semi-integral abutments). This report is intended to be a tool to the designers in the design of specific components and design detail recommendations that are intended to improve the durability performance of high skew bridges constructed with the link slabs and deck sliding over backwall or backwall sliding over the abutments.

## **1.2 PROJECT OBJECTIVES AND TASKS**

The objective of this project was to assess the performance and behavior of a high skew bridge structural system with link slabs and sliding deck over backwall or backwall sliding over abutment (semi-integral). The high skew bridge assessment was based on literature review, load testing, and analytical modeling and analysis. The project goal was to propose fine-tuning of the design assumptions and design details for the link slab and the abutment region.

The project tasks were as follows: (1) literature review, (2) assessment of skew bridge behavior under static truck loads and thermal expansion, (3) analytical and numerical analysis of skew link slabs, and (4) analytical and numerical analysis of skew sliding deck over backwall systems and semi-integral abutments.

## **1.3 REPORT ORGANIZATION**

The report is organized with 7 chapters.

- The Literature Review is presented in chapter 2 describing skew/jointless bridge behavior, modeling and analysis of skew bridge structural system/components, design and detailing of deck sliding over backwall and semi-integral abutments, and performance of jointless bridges.

- High skew bridge assessment under truck loads and thermal loads is presented in chapter 3.
- Chapter 4 describes skew link slab analysis and design.
- Chapter 5 describes skew abutment analysis and design.
- Chapter 6 presents the comprehensive results, recommendations, the need for further work, and
- Chapter 7 lists the references.

Intentionally left blank

## **2 STATE-OF-THE-ART LITERATURE REVIEW**

The objective of the literature review was to identify, review, and synthesize information related to skewed/jointless bridges. Finite element modeling of simply supported skewed bridges is also incorporated in various sections of the chapter to compare with and/or to benchmark the pertinent information available in literature. Concentration areas for the review are established for the project, and the following aspects will be discussed:

- Skewed bridge behavior under gravity loading,
- Skewed bridge behavior under volume change loads,
- Design challenges of skewed/jointless bridges, and
- Performance of skew/ jointless bridges.

### **2.1 OVERVIEW**

A skewed bridge is one in which the major axis of the substructure is not perpendicular to the longitudinal axis of the superstructure. The skew angle (most commonly in degrees) is defined as the angle between the axis normal to the bridge centerline and the axis along the abutment or pier cap centerline. Some highway agencies use a different convention. As an example, Michigan uses the angle of crossing which is the acute (small) angle formed between the longitudinal bridge axis and the abutment or pier cap centerline axis (Figure 2-1).

The majority of bridge decks built today have some form of skew, taper or curve. Because of the increasing restriction on available space for traffic schemes, the alignment of a transportation system can seldom be adjusted to reduce the skew. A skew angle greater than 20° alters the bending moment and shear developed in a bridge compared to those of a straight bridge. Skew bridge decks are prone to develop deck corner cracking (Fu et al. 2007).

About two-thirds of bridges nationwide are skewed (AASHTO LRFD 2010). According to the Pontis database, as of 2006, there are about 2,800 bridges in Michigan with a skew angle greater than 20° (Figure 2-2). This is in excess of 20 percent of the total bridge population of

12,691 bridges. Twenty percent of the concrete bridges and 30 percent of the steel bridges in Michigan's bridge inventory have a skew angle greater than 20° (Figure 2-3).

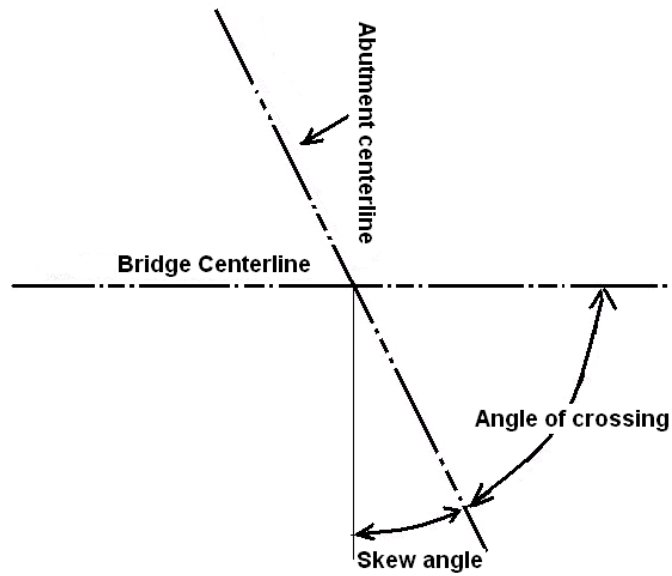


Figure 2-1. Geometric relation of skew angle and angle of crossing

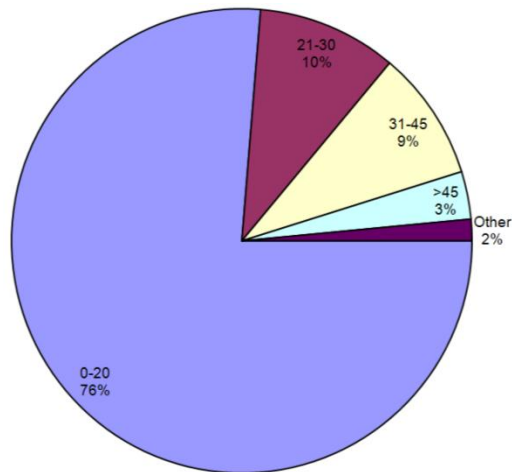


Figure 2-2. Percentages of skew bridges in Michigan

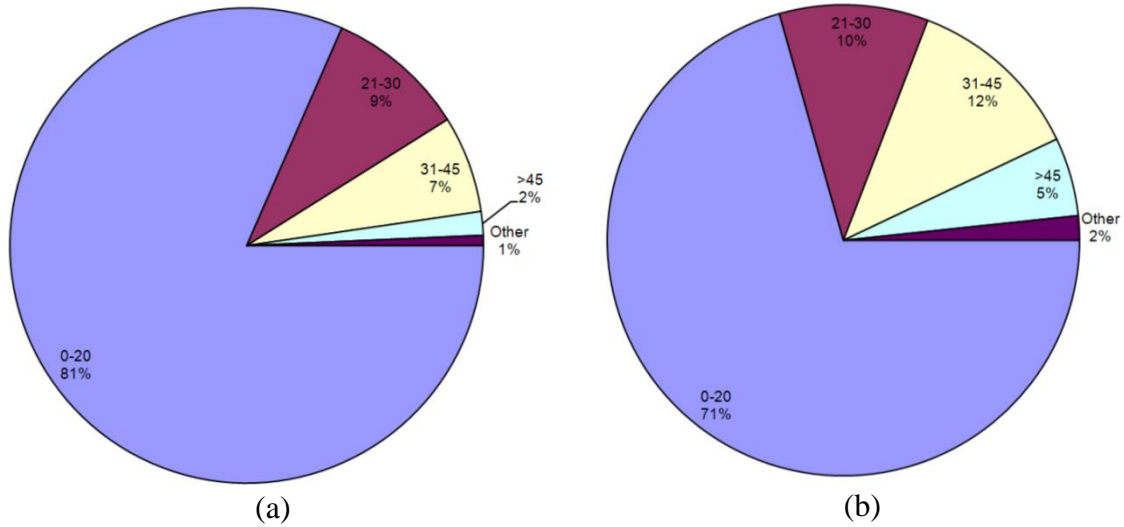


Figure 2-3. Percentage of skewed bridges in Michigan (a) concrete and (b) steel

## 2.2 SKEWED BRIDGE BEHAVIOR UNDER GRAVITY LOADING

In slab bridges and other bridges with high torsional rigidity, the load path develops between the obtuse ( $>90^\circ$ ) corners of the span (Figure 2-4). Longitudinal bending moments are reduced, but shear forces are increased in the obtuse corners (Figure 2-5). The special characteristics of the load response characteristics of a skewed solid slab bridge are summarized in Hambly (1991) as follows:

1. Variation in direction of calculated maximum bending moment across bridge width (Figure 2-5),
2. Hogging (negative) moments near obtuse ( $>90^\circ$ ) corner,
3. Torsion developing on the deck,
4. Larger reactions and shear forces near obtuse corner, and
5. Lower reactions and possible uplift in acute ( $<90^\circ$ ) corner.

The effects described above may also occur in stringer bridges, but they are much less pronounced. In stringer bridges, such as I- Tee- or bulb-tee beam bridges, the load tends to flow along the length of the supporting beams, and the effect of skew on the bending moments is reduced (Figure 2-4).

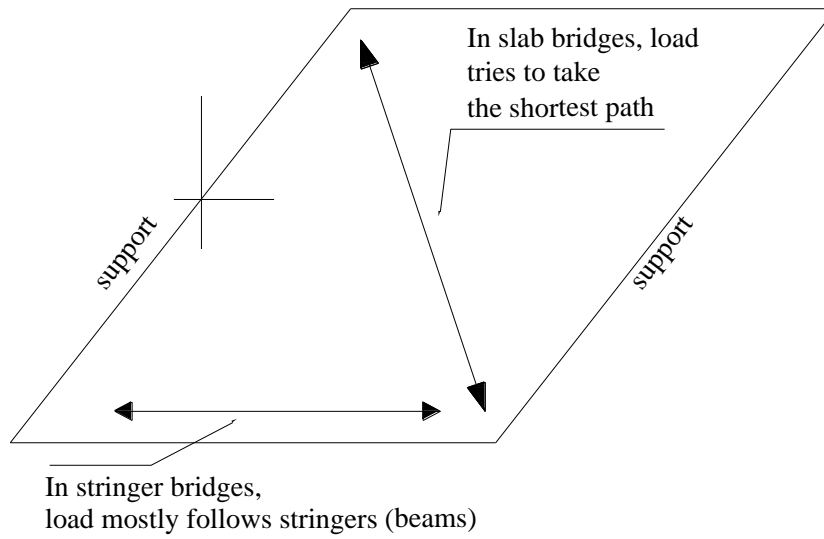


**Figure 2-4. Load distribution pattern in skewed stringer and slab bridges.**

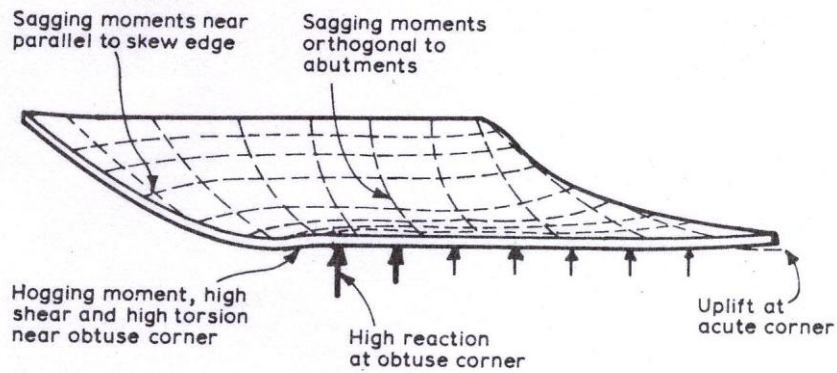


**Figure 2-5. Characteristics of skewed slab deck (Hambly 1991).**

Non-uniform girder end rotations of skew bridges under uniformly distributed load are observed across the bridge. If the torsional stiffness of the slab and girders is low, this distortion of deck may occur without creating large reaction forces. Under a concentrated load, beams behave similar to those of orthogonal bridges, and the load distribution still takes place by transverse bending of the slab. However, the increase in shear force and reaction at the obtuse corner may be significant and should be considered in girder and bearing design. Continuous decks may also exhibit large shear forces and reactions, particularly in the region of intermediate supports (Hambly 1991). The size of these effects depends on the skew angle, width to span ratio, and primarily on the type of deck construction and the supports.



### **2.2.1 Finite Element (FE) Simulation of Skew Bridge Behavior under Gravity Loading**

Finite element (FE) models are developed to evaluate the effects of various types and levels of loads on the behavior of simply supported skewed bridges. The primary aim in FE analyses is to develop a clear representation of the behavior of skewed bridges as presented in literature. Three-dimensional FE models are developed representing two major design categories: a solid slab bridge and a stringer bridge. A three-dimensional solid continuum brick element, which has three translational degrees of freedom at each node, is used to model bridge components (girders and deck). The analyses are particularly concentrated on stringer type bridges due to their significant presence.

The models developed for the analysis of skewed bridges are for a fictitious bridge with a span to width ratio of two (2). The span length is 63-ft 4-in. (760 in.) and the bridge width is 31-ft 8-in. (380 in.). The stringer bridge has five PCI Type III interior girders with a nine inches thick concrete deck (Figure 2-6). The span and width of the solid slab bridge are identical to the stringer bridge. A solid slab bridge with the current dimensions would neither meet the strength nor service requirements. However, the primary aim in these analyses is to demonstrate the skew effects. The bridges are constrained so that one end would be free for longitudinal movement. The other end would be restrained in the longitudinal and vertical directions with only the center node pinned in all three translational directions as shown in Figure 2-7. Skew angle is varied between zero and 60°. Resulting moment outputs are obtained at multiple points along the lines parallel to the skewed edge (Figure 2-7). Moment resultants are obtained for the full-width of the structure. In the case of stringer bridges, individual girder moments are not obtained since the primary aim is not set towards live load distribution.

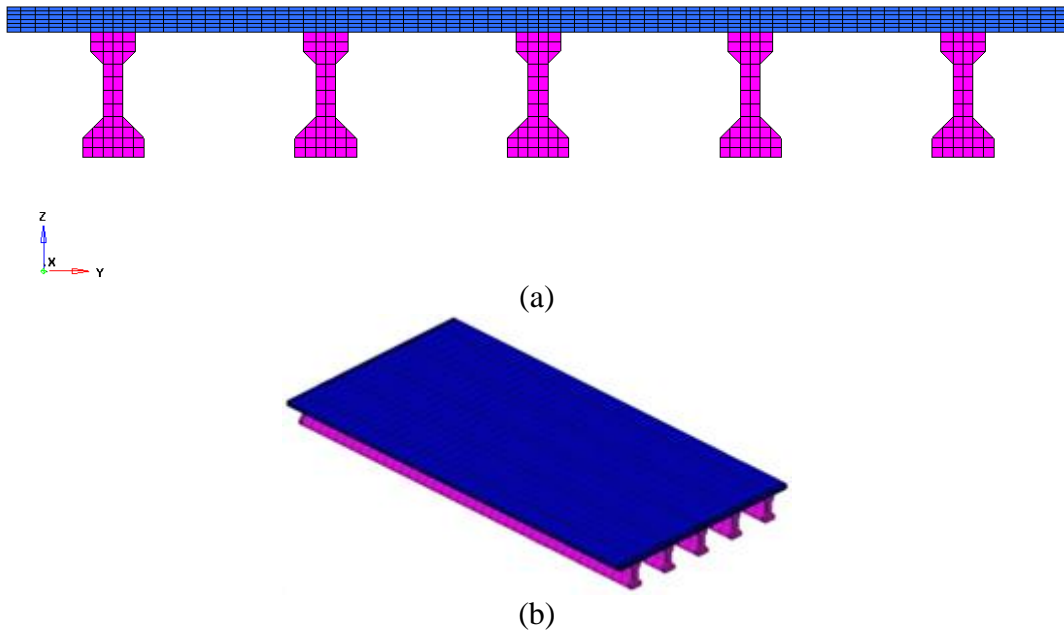


Figure 2-6. (a) Cross section and (b) isometric views of the stringer models

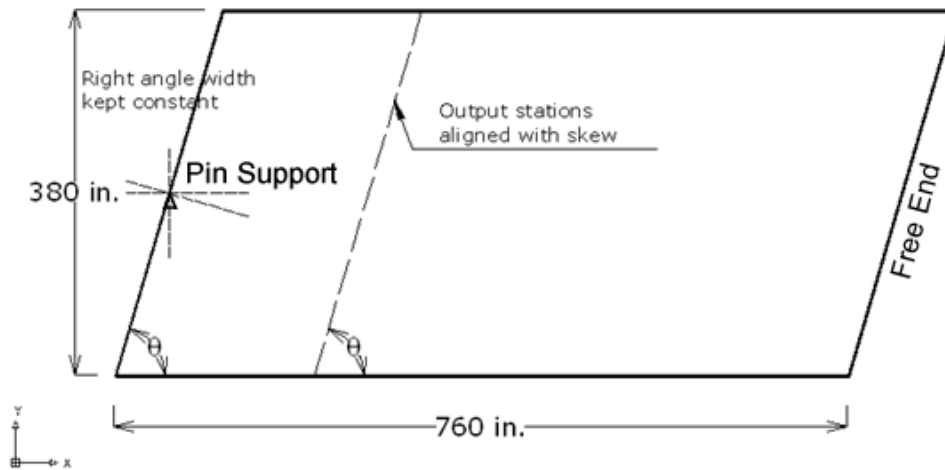


Figure 2-7. Plan view of FE models

Deck and girder design strengths are different in various states throughout the U.S. The Michigan Department of Transportation (MDOT) requires a minimum compressive strength of the girder and deck concrete of 4500 psi. This is the value used to calculate the concrete modulus as per AASHTO LFRD (2010) Section 5.4.2.4 for the FE models. Poisson's ratio of 0.2 is used for both deck and girder concrete. Unit weight of concrete is taken as 150 lb/ft<sup>3</sup>. Two independent load cases are considered: self-weight and a concentrated load of 50 kips that is placed at the center of mid-span.

### *2.2.1.1 Analysis Requirements of Simple Span Skew Bridges*

Menassa et al. (2007) investigated the effects of different skew angles on reinforced concrete slab bridges. Ninety-six bridge configurations were developed and analyzed considering various geometric bridge characteristics including the span length and slab width with six different skew angles. FE analyses results of skewed bridges were compared to the reference straight bridges as well as the AASHTO Standard Specifications and LRFD procedures. Under live load, maximum longitudinal moment decreased, whereas, maximum transverse moment increased with increasing skew angles. The variation in moment was significant for skew angles greater than  $20^\circ$ . The research concluded that skew angles less than or equal to  $20^\circ$  can be designed as a straight bridge. This conclusion complies with the AASHTO Standard and LRFD (2002 and 2010). Menassa et al. (2007) recommended using three-dimensional finite element analysis for bridges with a skew angle greater than  $20^\circ$ .

The skew policy described in the MDOT Bridge Design Manual (MDOT 2005) section 7.01.14 requires special design by refined analysis methods for bridges with skew greater than  $30^\circ$  but equal or less than  $45^\circ$ . Further, if the skew is greater than  $45^\circ$ , refined analysis as well as special approval through bridge design is required.

### *2.2.1.2 FE Simulation of Simple Span Skew Bridges under Gravity Loads*

Finite element analyses results are utilized to make a comparison with the available literature on skewed bridges. First, a brief comparison between the stringer and solid slab type bridges is presented, and then detailed results are provided only for the stringer type bridges.

The transverse bending stress (stress Y-Y) distribution of stringer and solid slab type bridges under self-weight are shown in Figure 2-8 which agrees with the representation of the load path depicted in Figure 2-4. Figure 2-9 shows only the negative (hogging) longitudinal bending stress regions under self-weight for the two different bridge types. Hogging (negative) moment regions are displayed near obtuse corners. The general effects of gravity loading, i.e., decreased longitudinal moments, high shear and reactions in obtuse corners, can be seen under both dead and concentrated load.

Longitudinal bending moment plots for stringer type bridges are given in Figure 2-10 and Figure 2-11 under self-weight and concentrated loads, respectively. The longitudinal bending moment decreases nonlinearly with an increasing skew angle, irrespective of the load type (Figure 2-12). The bending moments decrease by about 13 and 19 percent with an increased skew from 0° to 60° under self-weight and concentrated loads, respectively. Straight simply supported bridges do not develop any torsion under symmetrical gravity loading. However, with skew, significant torsion of the deck is generated. Torsion distribution along the length of the stringer bridge for different skew angles is shown in Figure 2-13 and Figure 2-14 under self-weight and concentrated loads, respectively. Torsion is constant apart from the supports and increases with increasing skew angle. Support Reaction variations for obtuse and acute corners are presented in Figure 2-15 under self-weight. The reaction force in the obtuse corner increases by up to 30 percent, whereas a 10 percent decrease is observed in the acute corner when skew angle is increased from 0° to 60°.

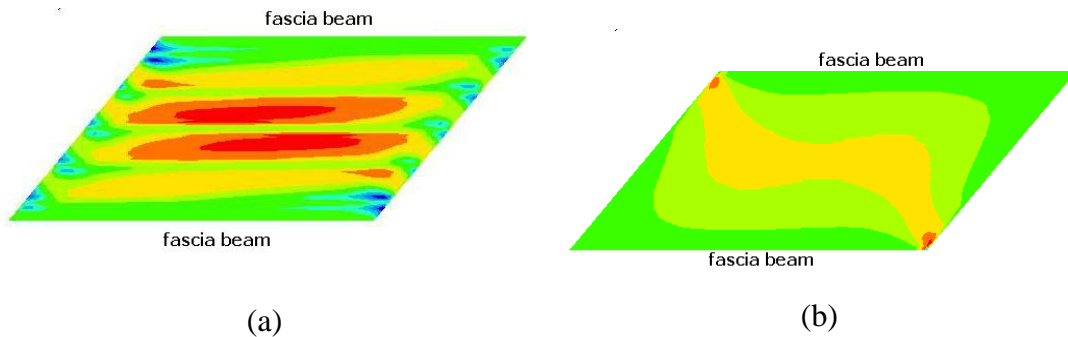


**Figure 2-8. Transverse bending stress distribution of deck for (a) stringer bridge deck and (b) solid slab for 40° skew under self-weight**

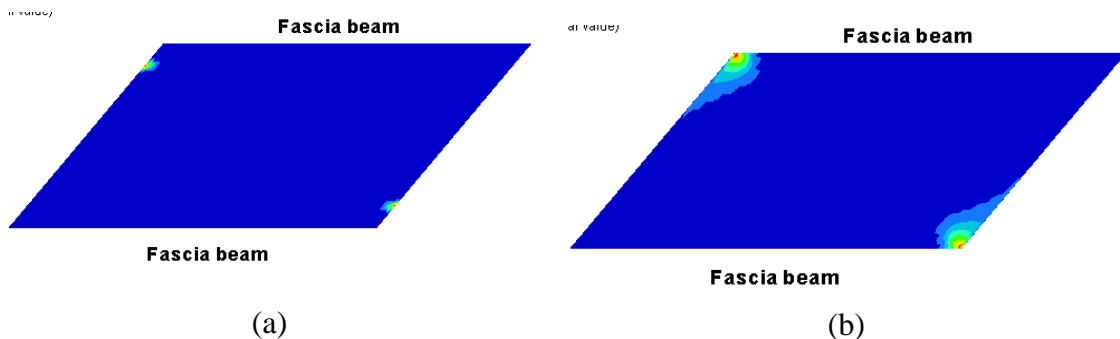


**Figure 2-9. Longitudinal bending stress distribution (a) stringer (b) solid slab bridge of 40° skew under self-weight (negative moment regions only)**

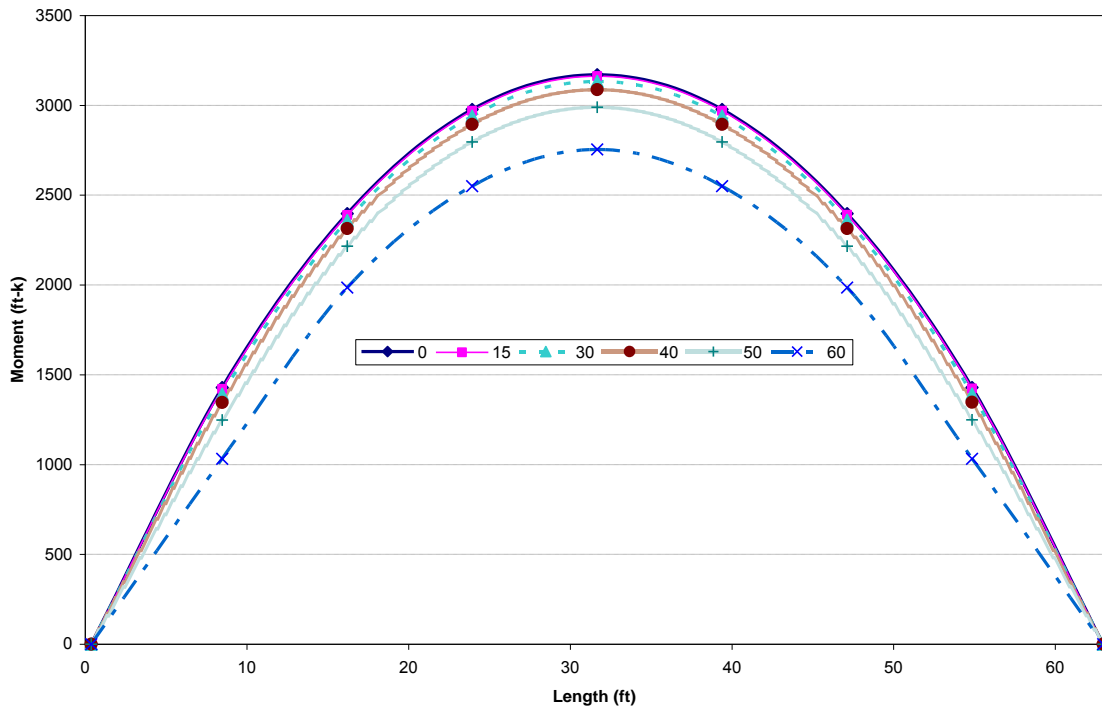


**Figure 2-10. Longitudinal bending moment variation against skew for full-width stringer bridge under self-weight**

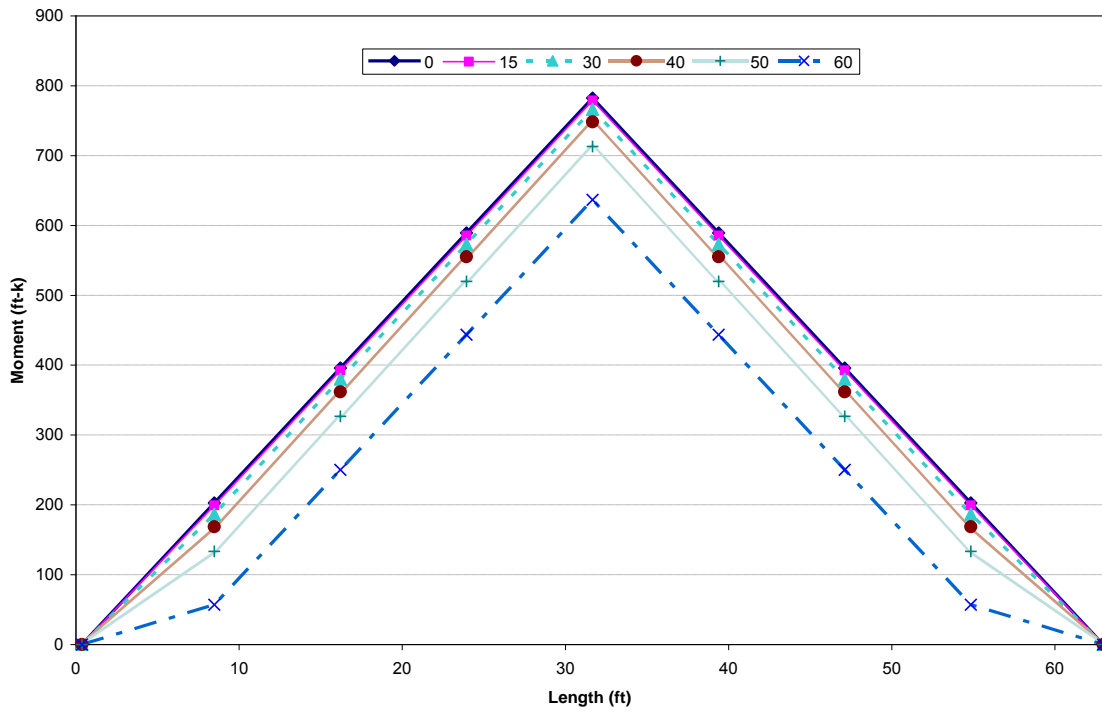


**Figure 2-11. Longitudinal bending moment variation against skew for full-width stringer bridge under a concentrated load**

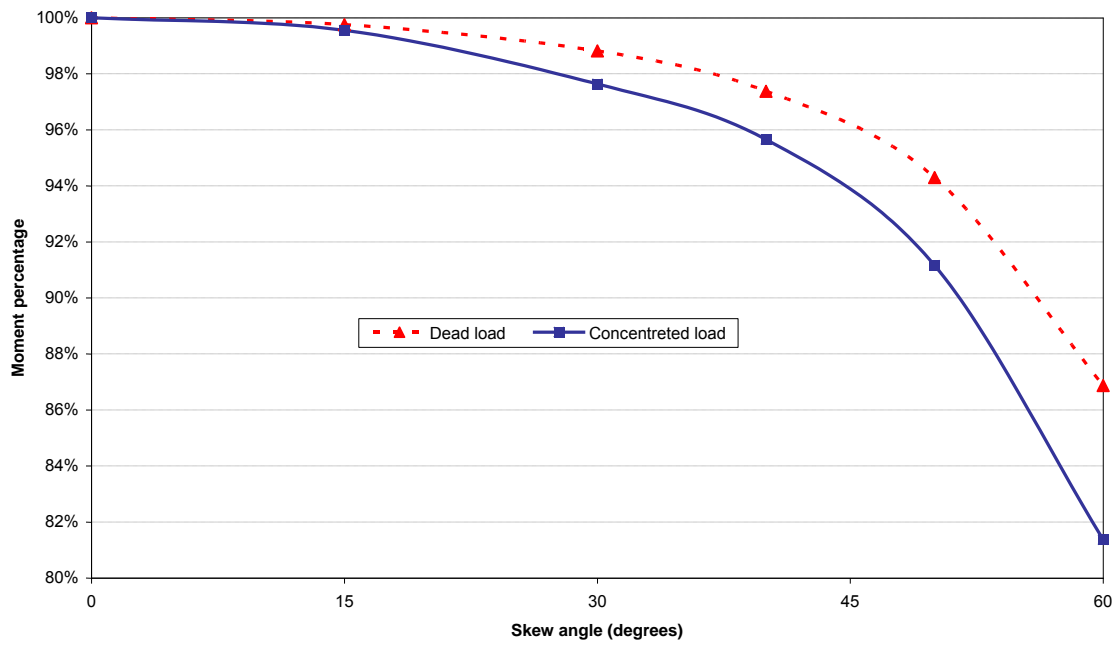


**Figure 2-12. Mid-span moment variation vs. skew angle under self-weight and concentrated load for stringer bridge**

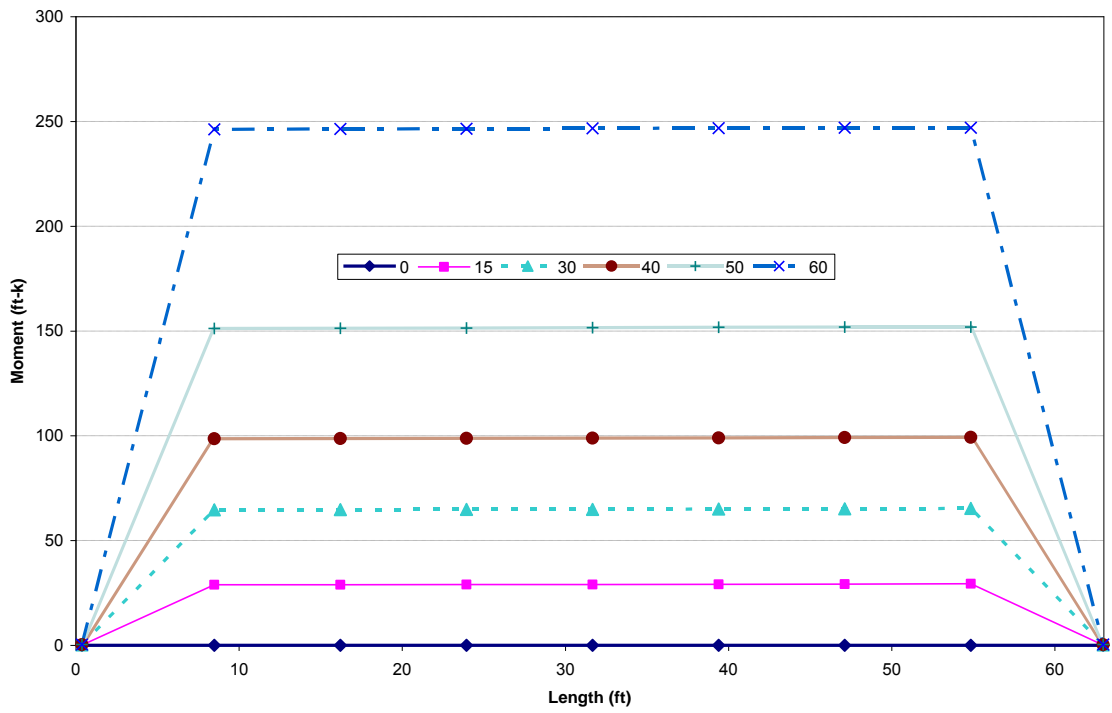


**Figure 2-13. Torsion for full-width of stringer bridge under self-weight**

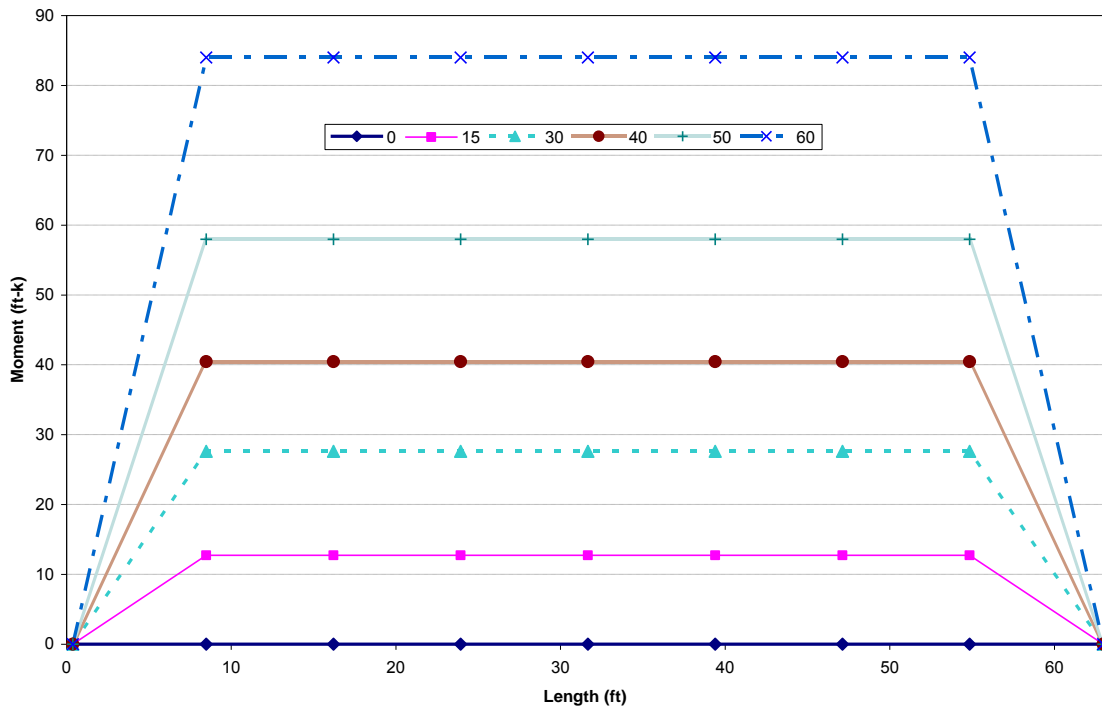


Figure 2-14. Torsion for full-width of stringer bridge under concentrated load

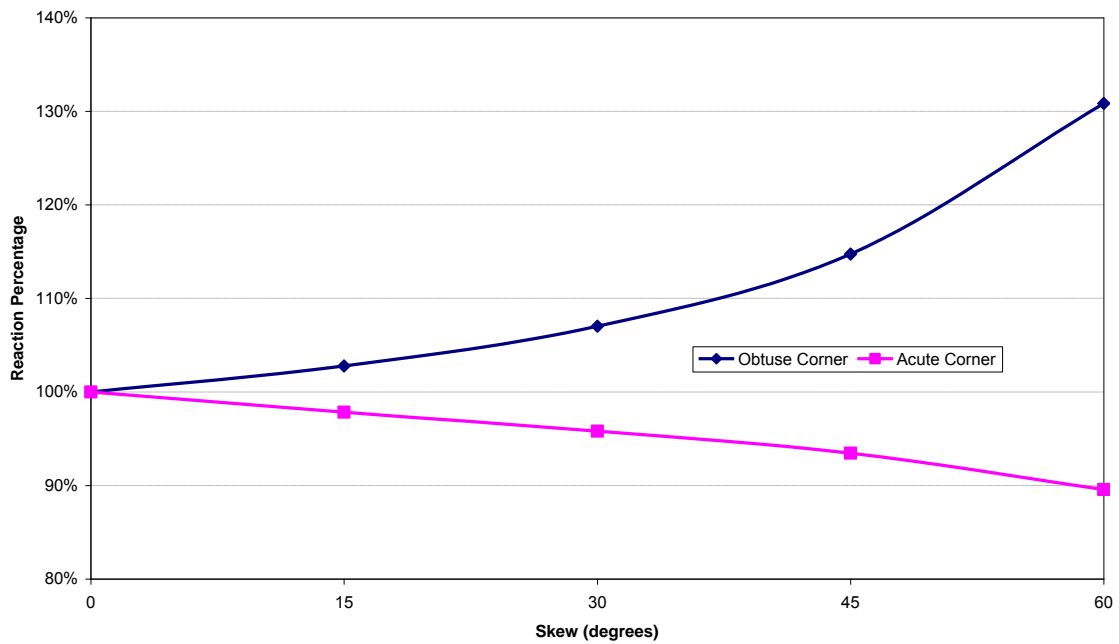
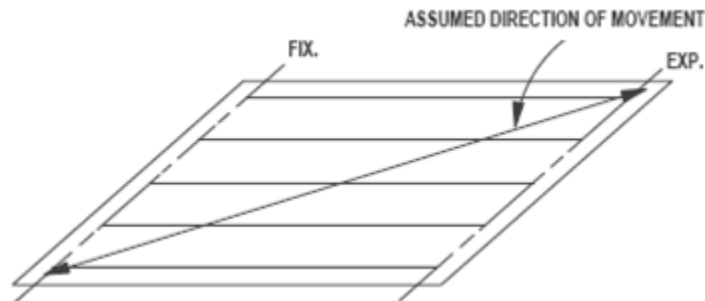


Figure 2-15. Support reaction vs. skew angle for stringer bridge under self-weight

### 2.3 SKEWED BRIDGE BEHAVIOR UNDER VOLUME CHANGE LOADS

Skewed bridges exhibit a complex response pattern under volume change loads with regard to both bearing deformations and restraint forces. Transverse movement is generated in wider bridges that tend to rotate with respect to the vertical axis. Restraint forces vary considerably with skew and show nonlinear behavior (Tindal and Yoo 2003). The direction of movement and rotation of bearings for curved and high skew bridges depends on many factors and is not easily determined. However, the major axis of thermal movement on a high skew bridge is most generally along the diagonal between the acute corners (Figure 2-16). The alignments of the bearings and layout of the keeper blocks parallel to the axis relieve all the stresses; yet implementation is not very practical (AASHTO LRFD 2010).



**Figure 2-16. Direction of skew simply supported bridge movement under uniform thermal load**

Round bearings are recommended for curved and high skew bridges since they can accommodate movement and rotations in multiple directions. Round bearings also require a narrower bridge seat on skew bridges (Najm et al. 2007).

According to a survey conducted by Najm et al. (2007), eight out of 39 state DOTs (21%) have used round bearings. Eighteen states (46%) were willing to consider using them. Agencies have used round bearings on curved and high skew bridges, and on pier caps with limited space. According to the survey results, 29% of the round bearing applications were for mild skew bridges, 50% for high skew, and 21% for curved bridges. As for bridge length and type, most of the bridges with round bearings have spans less than 115 ft long, and two-thirds of these bridges were precast concrete girder bridges while the remaining were steel stringer .



An FHWA study conducted by Yazdani and Green (2000) showed that the effect of increasing bearing stiffness is both beneficial and detrimental to the skew bridge system depending on boundary conditions. Bearing pads with a higher shear modulus will reduce midspan deflection in high skew bridges. Intermediate diaphragms also reduce overall midspan deflection and maximum stresses; yet the reductions were smaller for high skew bridges. Deflections would decrease by about 17% for straight bridges, but only about 5% for 60° skew bridges when intermediate diaphragms are used.

There are various bearing orientations discussed in literature (Tindal and Yoo 2003) that allow transverse movement as shown in Figure 2-17. In the traditional case, bearings are fixed both longitudinally and transversely at one end allowing expansion at the opposite end, only in the longitudinal direction (Figure 2-17a). In other alternatives, a single bearing at the corner (Figure 2-17b) or at the center (Figure 2-17c) of one end is restrained allowing rest of the bearings to expand or contract freely in both longitudinal and transverse directions. It should be noted that for cases where only single bearing is restrained (radial from corner or radial from center), longitudinal or transverse bearing forces will not develop under uniform strain (i.e., under uniform thermal loading). However, under thermal gradient load, transverse bearing forces will develop.

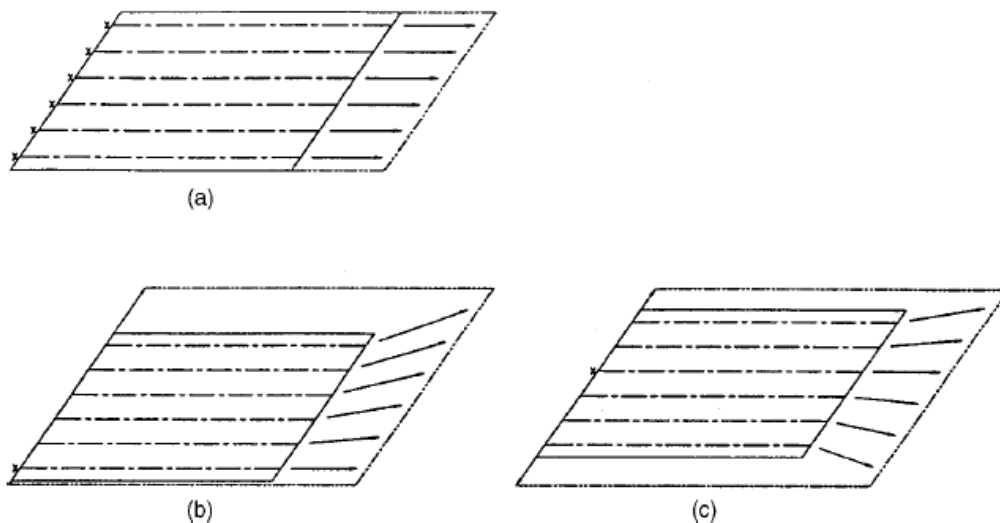


**Figure 2-17. Bearing orientation for constraint cases (a) traditional, (b) radial from corner, (c) radial from center (Tindal and Yoo 2003)**

Tindal and Yoo (2003) performed a parametric study investigating all three constraint configurations shown in Figure 2-17 for simply supported skew bridges under both winter and summer thermal loads. It should be noted that, although not explicitly stated in the study, in order to achieve the expansion profiles shown in Figure 2-17, expansion bearings should have guided plates to facilitate deformations in the direction of reference line. If the expansion bearings were only vertically restrained, the expansion profile would also change and follow a more random pattern. This behavior is further investigated and will be discussed later in this chapter.

Tindal and Yoo (2003) also investigated the effect of thermal gradient loading. A uniform temperature profile was imposed through the girder depth and linearly increasing profile along the deck thickness. Restraint forces at bearings varied considerably with skew angle. Restraint force trends for all cases were nonlinear and showed substantial differences. In both radial from corner and radial from center cases, bearing forces substantially reduced for all skew angles. Bearing orientation, shown in Figure 2-17b, performed best for skew angles less than  $20^\circ$  and greater than  $55^\circ$ , whereas the orientation shown in Figure 2-17c performed better for intermediate skew angles. Skewed bridges developed large bearing forces under the traditional bearing configuration (Figure 2-17a), which would explain the tendency of the bridges to rotate about their supports (i.e., about the vertical axis of a bridge). Under the traditional and the radial from corner bearing orientations, maximum reaction was always at the acute angle of the fixed end. This was not always the case for radial from center bearing orientation.

Moorthy and Roeder (1992) performed a parametric study considering skew angle, width and length, and the expansion joint and bearing pad characteristics of a bridge. A three-span, composite, continuous steel-girder bridge was used as the primary structural system. Girder translations were fixed with pin bearings on one abutment, whereas beams were supported on rocker bearings on all other supports that restrained transverse translations. The bridge included expansion joints at both abutments. A thermal gradient load was applied with a nearly uniform profile along the height of the girder while varying nonlinearly about  $20^\circ\text{F}$  through the concrete deck. The resulting longitudinal displacements of the straight bridge were uniform across the width. With increasing skew, maximum longitudinal displacements

were calculated along the diagonal between acute corners (Figure 2-18). The transverse displacements of the straight bridge were symmetrical about the longitudinal axis. With increasing skew, maximum transverse displacements were obtained along the diagonal between acute corners (Figure 2-19). A comparison of normalized longitudinal and transverse displacements with respect to skew angle is also shown in Figure 2-20. Longitudinal and transverse displacements increased with increasing skew. The increase in transverse displacements of the deck generated girder torsional rotations along the longitudinal axis. This was because the girder bottom flanges were restrained for transverse movement while the girders and the deck were rigidly connected. Transverse movements are particularly damaging since the bridge is restrained in that direction. This is especially critical to relatively short and wide bridges because of their higher rotational stiffness.

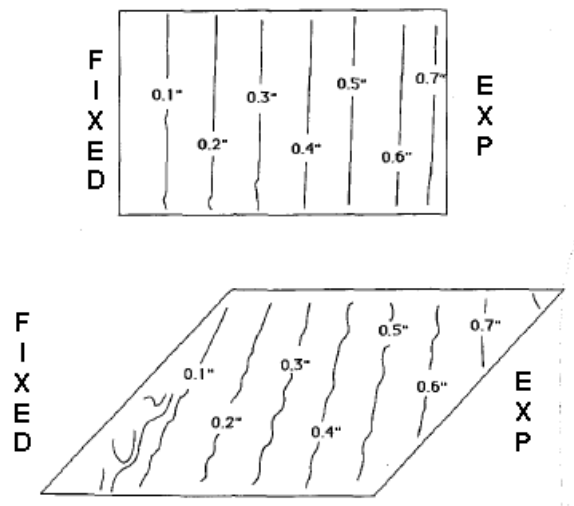


**Figure 2-18. Longitudinal displacement profile of deck for right and 45° skew bridge (Moorthy and Roeder 1992).**

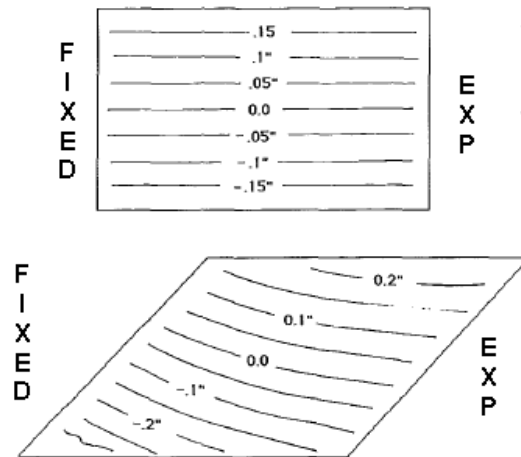


Figure 2-19. Transverse displacement profile of deck for right and 45° skew bridge (Moorthy and Roeder 1992).

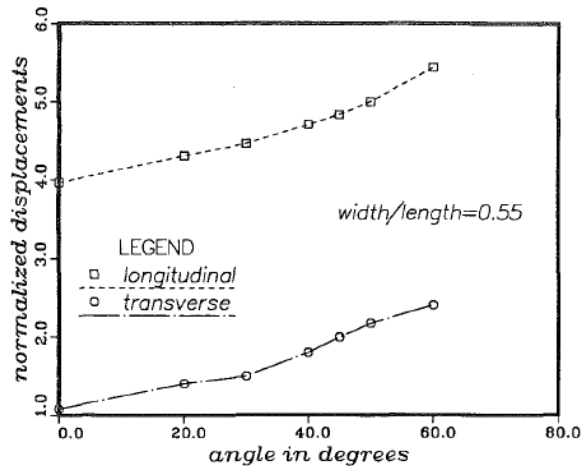
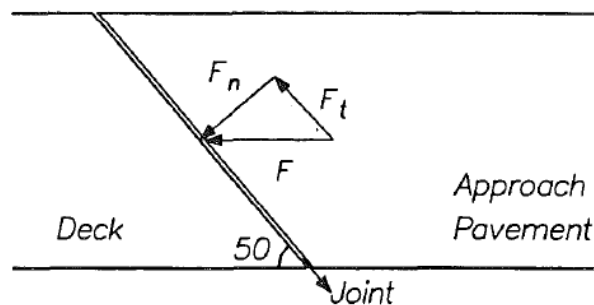


Figure 2-20. Maximum normalized longitudinal and transverse displacement vs. skew angle (Moorthy and Roeder 1992).

Moorthy and Roeder (1992) investigated the effects of bearing resistance to the longitudinal movement. According to the study, the rocker bearings did not move until a threshold slip force was reached and moved freely afterwards. The effect of resistance to longitudinal movement, provided by the bearings and expansion joints, was examined by changing the slip force between 0 and 80% of the self-weight reaction force acting on the bearing. As the bearing slip force was increased, there was an increase in transverse movement along the diagonal between acute corners. Also, the forces in the girders and bearings increased considerably. The resistance of expansion joints to the longitudinal movement increased

transverse movement as well as the deck and bearing stresses while reducing the longitudinal movement. The study recommended use of elastomeric bearings or those with unguided sliding surfaces for high skew, short, and wide bridges since the potential transverse movement was permitted.

Moorthy and Roeder (1992) stated that resistance encountered in expansion joints or support locations can considerably increase the transverse movement in skew bridges. Compressive reaction force,  $F$ , is developed across the skew angle as shown in Figure 2-21. Compressive force,  $F_n$  is developed in the normal direction due to limited shear strength between pavement and the granular base. The transverse component  $F_t$ , will push the bridge transversely which may generate larger transverse movements in the absence of bearing guides or other transverse restraints.



**Figure 2-21. Forces on deck due to resistance encountered in expansion joints (Moorthy and Roeder 1992).**

Moorthy and Roeder (1992) investigated the effects of pier stiffness. The pier stiffness did not have a great impact on the movements noted for relatively short skew bridges that experience large transverse movements but had a notable impact on longer bridges.

### 2.3.1 Skew Bridge Behavior under Thermal Loads

The skew bridge behavior is analyzed under uniform thermal as well as positive and negative thermal gradient loads. Thermal gradient loads from AASHTO LRFD (2010) Section 3.12.3 for Zone-3 are used. A negative temperature gradient (NTG) is obtained by multiplying the positive temperature values by -0.30. The height ( $h$ ) in Figure 2-22 is the depth of full composite section (45 in. = 36 in. girder + 9 in. deck). A thermal expansion coefficient of  $6.0 \times 10^{-6}/^{\circ}\text{F}$  is used for both deck and girder concrete. Uniform expansion and contraction

temperature differentials of +42.3 °F and -72.7 °F are used as uniform thermal loads as per AASHTO LRFD Procedure B. Temperature gradient and uniform thermal loads are applied only to stringer bridge models.

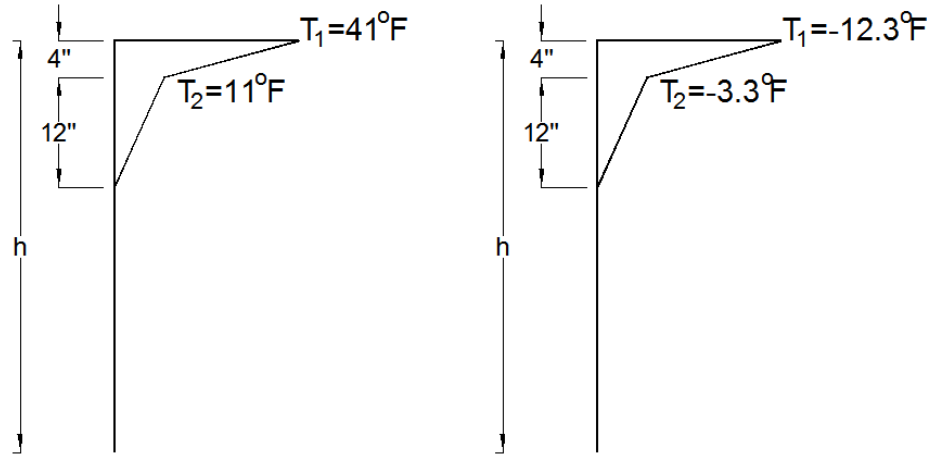


**Figure 2-22. Positive and negative temperature gradient loads used in the analyses**

### 2.3.1.1 FE Simulation of Simple Span Skew Bridge Behavior under Uniform Thermal Loads

To verify the findings documented in the literature, FE models of a simply supported stringer bridge are developed for skew angles of 0, 15, 30, 45 and 60 degrees. The models were analyzed under a uniform contraction thermal load for three different bearing orientations shown in Tindal and Yoo (2003). Traditional bearing systems limit the supports to move only along the longitudinal axis of the bridge. Radial from corner and radial from center bearing systems allow a movement pattern along the diagonal between acute corners as shown in Figure 2-23, Figure 2-24, and Figure 2-25. In these analyses gravity loads are not applied; that is, the displacement contours represented show the translations in longitudinal and transverse directions. Findings shown in Figure 2-24, Figure 2-25, and Figure 2-26 are in agreement with what is described in AASHTO Steel Bridge Bearing Design and Detailing Guidelines (AASHTO 2004, Figure 2-16). Radial from single bearing orientations (radial from corner and radial from center) are determinate systems and do not develop any reaction forces or stresses under uniform thermal load. However, the traditional bearing system experiences high reactions as well as stresses at the fixed end. The girder ends at the fixed end may also rotate developing girder torsion (Figure 2-26, Figure 2-27, and Figure 2-28).

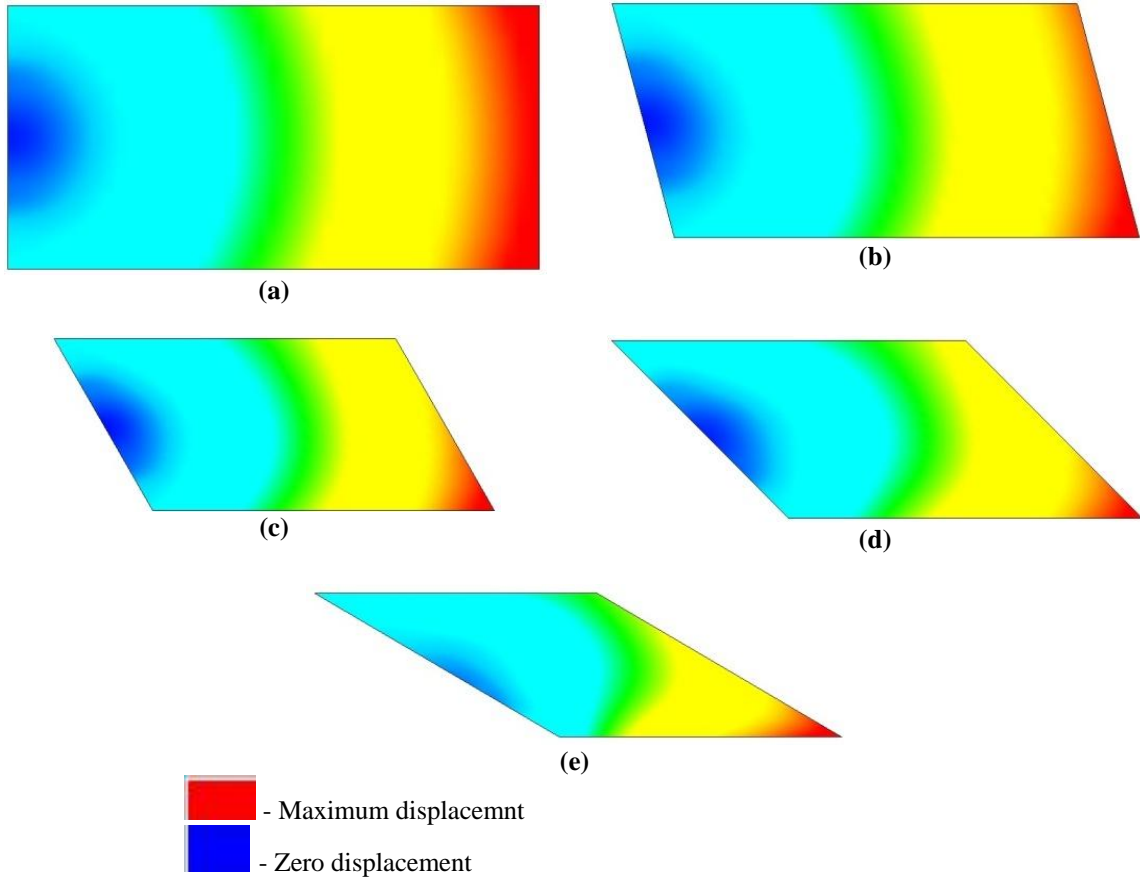


**Figure 2-23. Displacement contours under the traditional bearing condition for skew angles**  
 (a) 0° (b) 15° (c) 30° (d) 45° (e) 60°

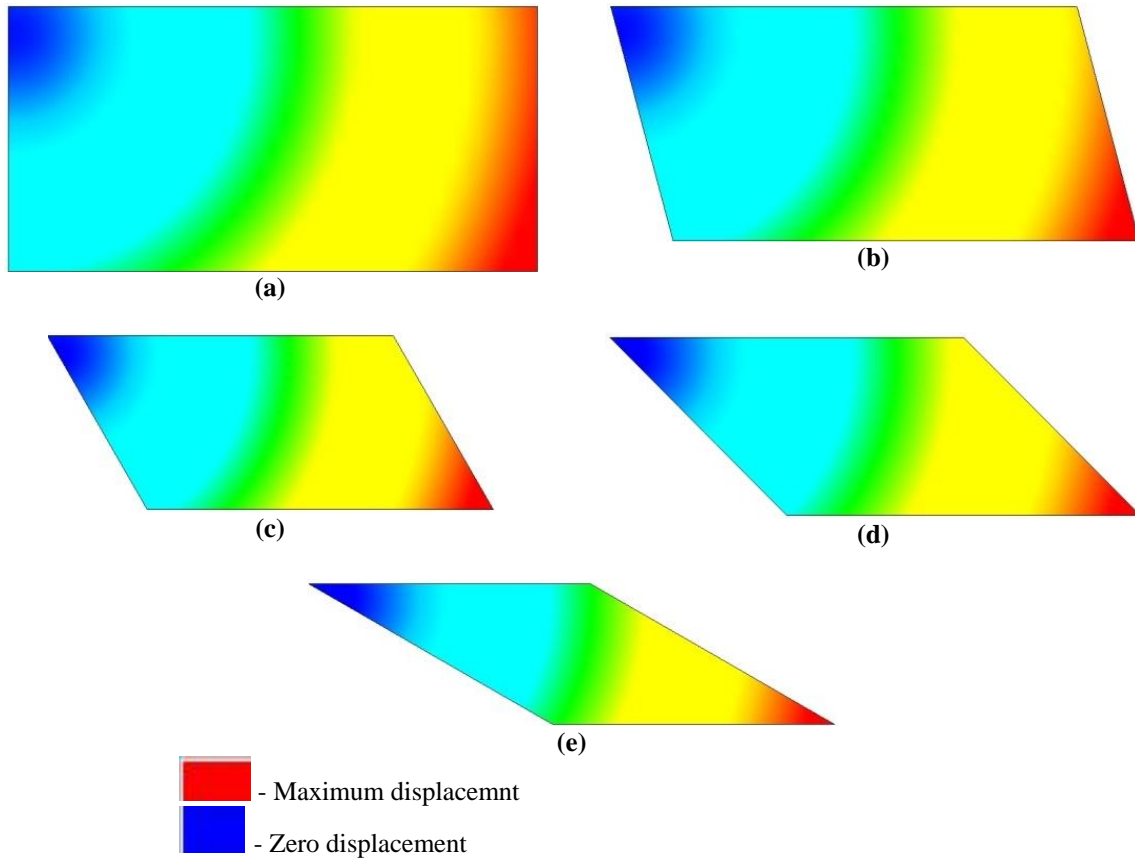


**Figure 2-24. Displacement contours under radial from corner bearing condition for skew angles**  
 (a) 0° (b) 15° (c) 30° (d) 45° (e) 60°



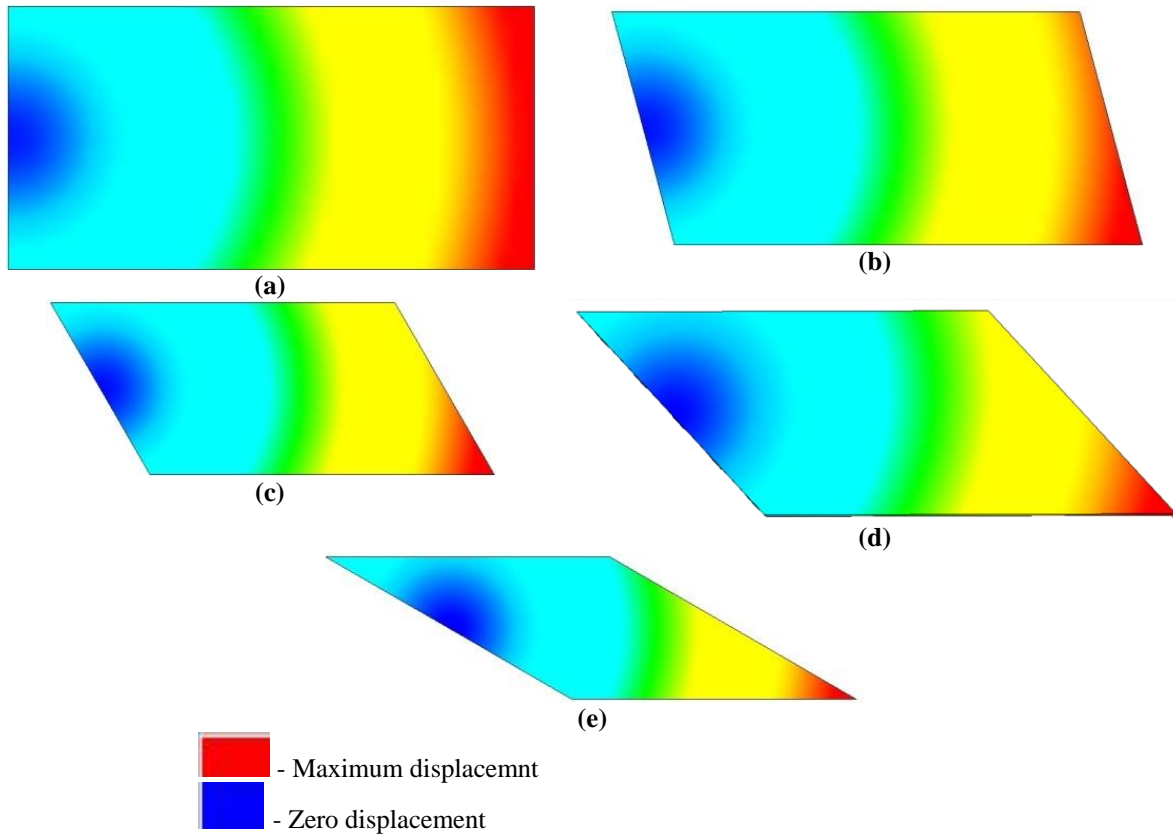


**Figure 2-25. Displacement contours under the radial from center bearing condition for skew angles**  
 (a) 0° (b) 15° (c) 30° (d) 45° (e) 60°

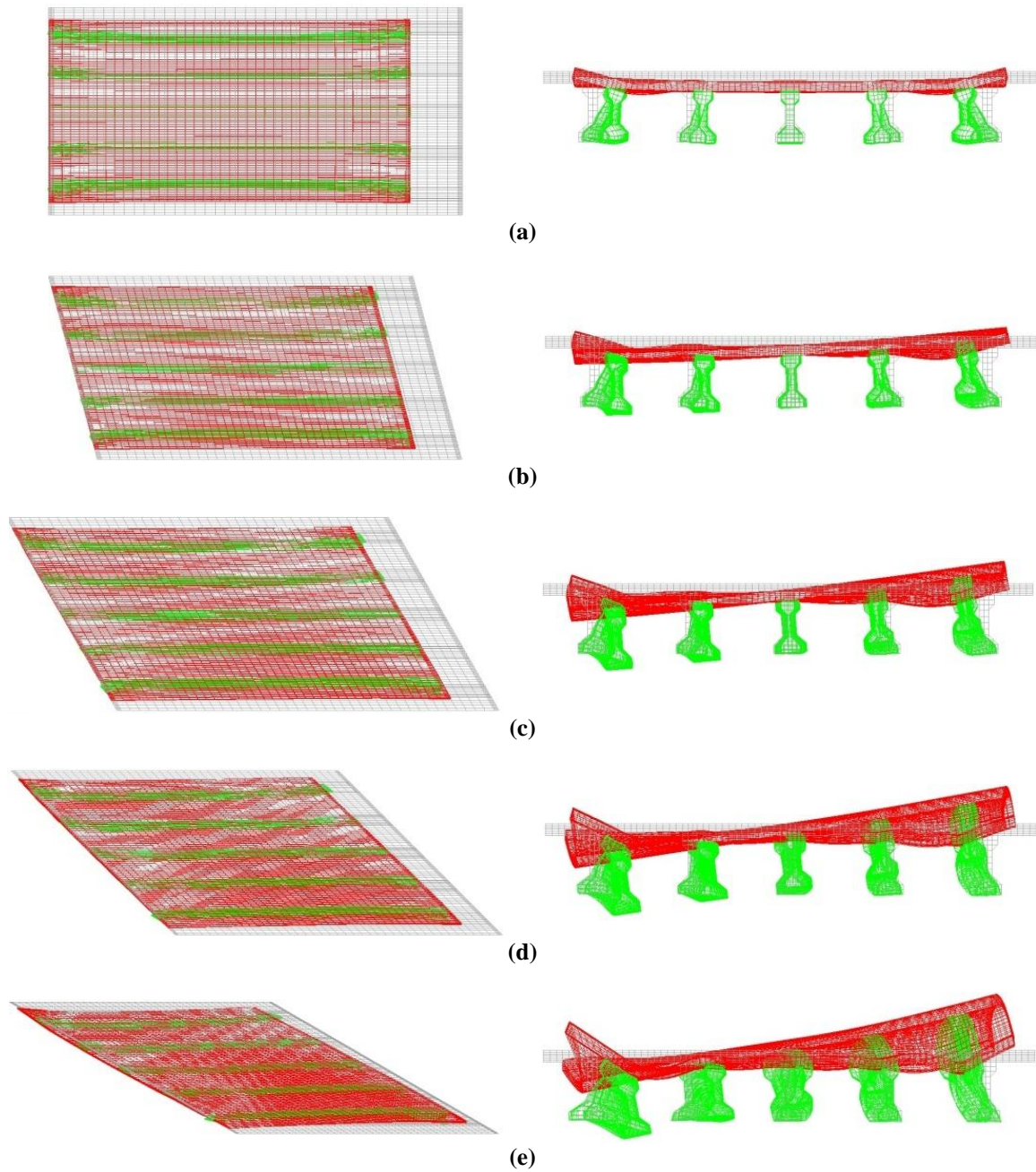


**Figure 2-26. Deformed shape under the traditional bearing condition for skew angles  
 (a) 0° (b) 15° (c) 30° (d) 45° (e) 60°**

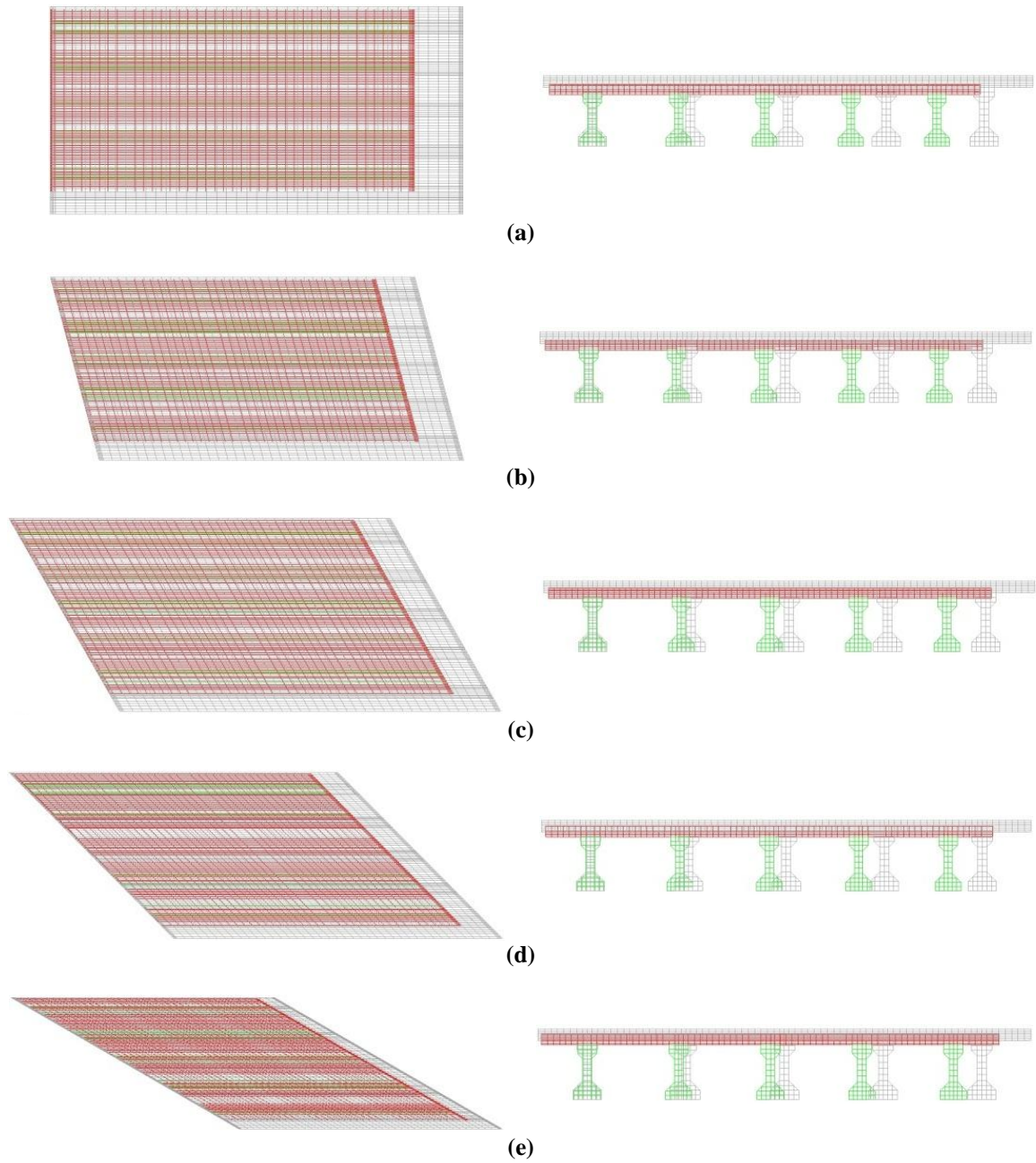


**Figure 2-27. Deformed shape under radial from corner bearing condition for skew angles**

(a) 0° (b) 15° (c) 30° (d) 45° (e) 60°

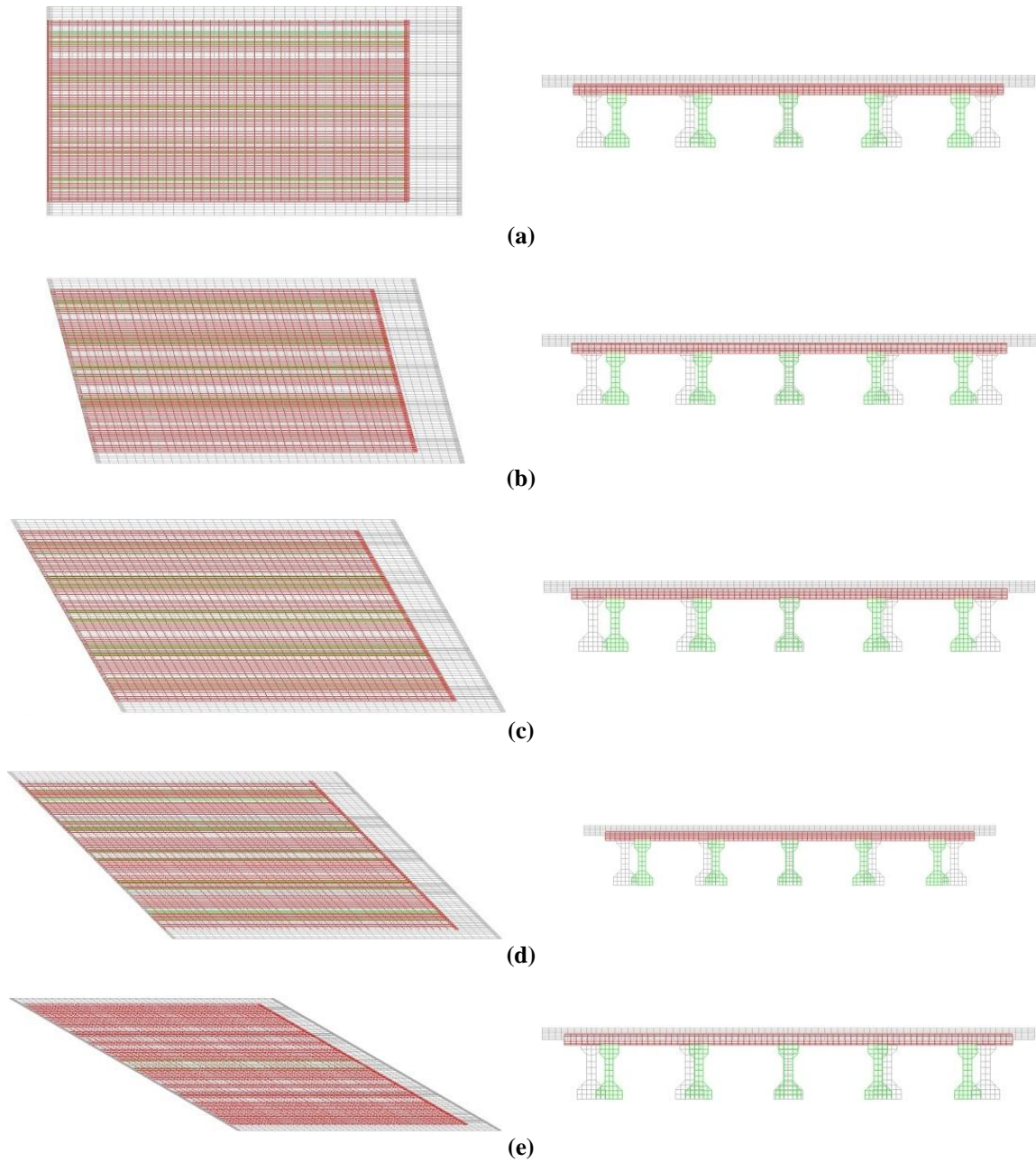


**Figure 2-28. Deformed shape under radial from center bearing condition for skew angles**

**(a) 0° (b) 15° (c) 30° (d) 45° (e) 60°**

Displacement contours in transverse and longitudinal directions are shown separately so that they can be compared with those of Moorthy and Roeder (1992). Figure 2-29, Figure 2-30, and Figure 2-31 show the displacement contours in transverse and longitudinal directions under three different bearing configurations. Irrespective of support configurations, maximum longitudinal bearing movement is at the acute corner. In traditional bearing configuration, longitudinal movement of the bridge is almost parallel to the angle of crossing (i.e., maximum movement at the acute corner and the minimum at the obtuse corner). In the radial cases, the longitudinal displacement contours are almost perpendicular to the diagonal between acute corners. As bridge skew increases, the direction of transverse displacement contours of bridge with traditional bearings changes from parallel to longitudinal axis to parallel to the diagonal between obtuse corners. In the case of radial bearing configuration, transverse displacement contours are parallel to the longitudinal axis of the bridge. The contraction (or expansion) profiles of the three different constraint cases do not follow the reference lines, and the deformed shapes do not resemble the ones previously shown in Figure 2-17. Thus, guided bearings that would allow movement along the reference line are necessary to achieve the expansion profiles shown in Figure 2-17. The same behavior is also discussed in Nakai and Yoo (1988), but no design details are provided.

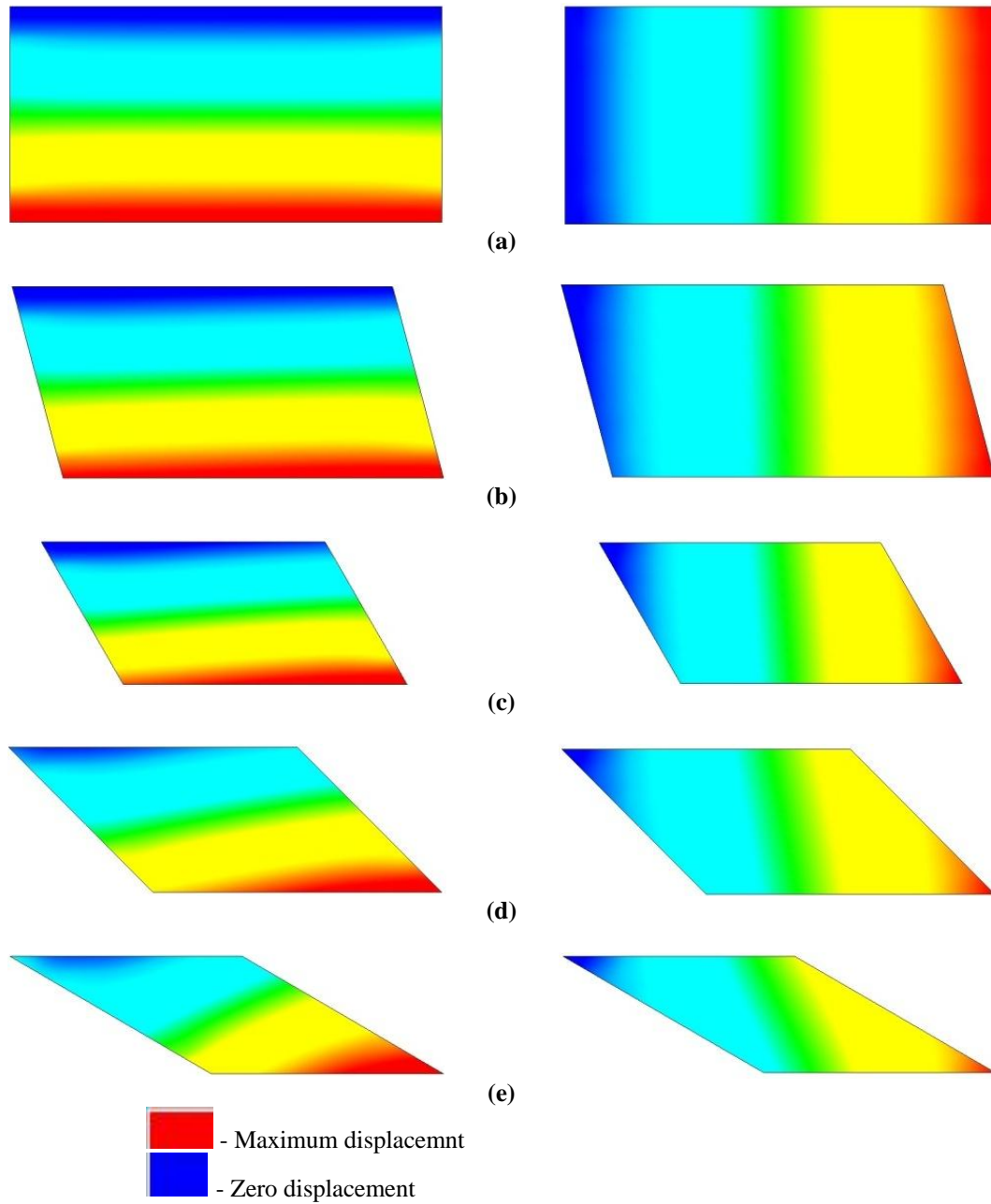


**Figure 2-29. Transverse (left) and longitudinal (right) displacement contours under the traditional bearing condition for skew angles (a) 0° (b) 15° (c) 30° (d) 45° (e) 60°**

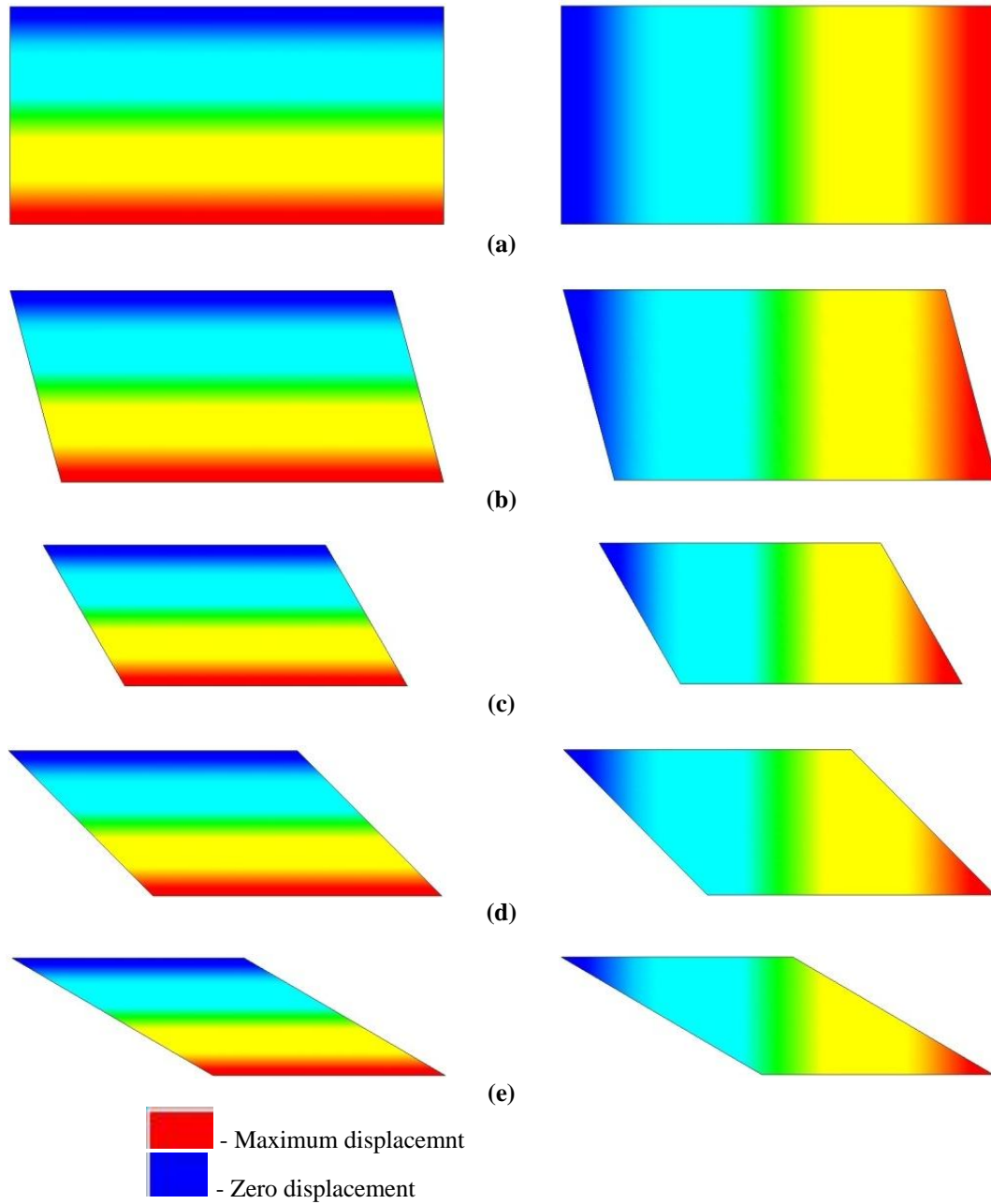


**Figure 2-30. Transverse (left) and longitudinal (right) displacement under the radial from corner bearing condition for skew angles (a) 0° (b) 15° (c) 30° (d) 45° (e) 60°**

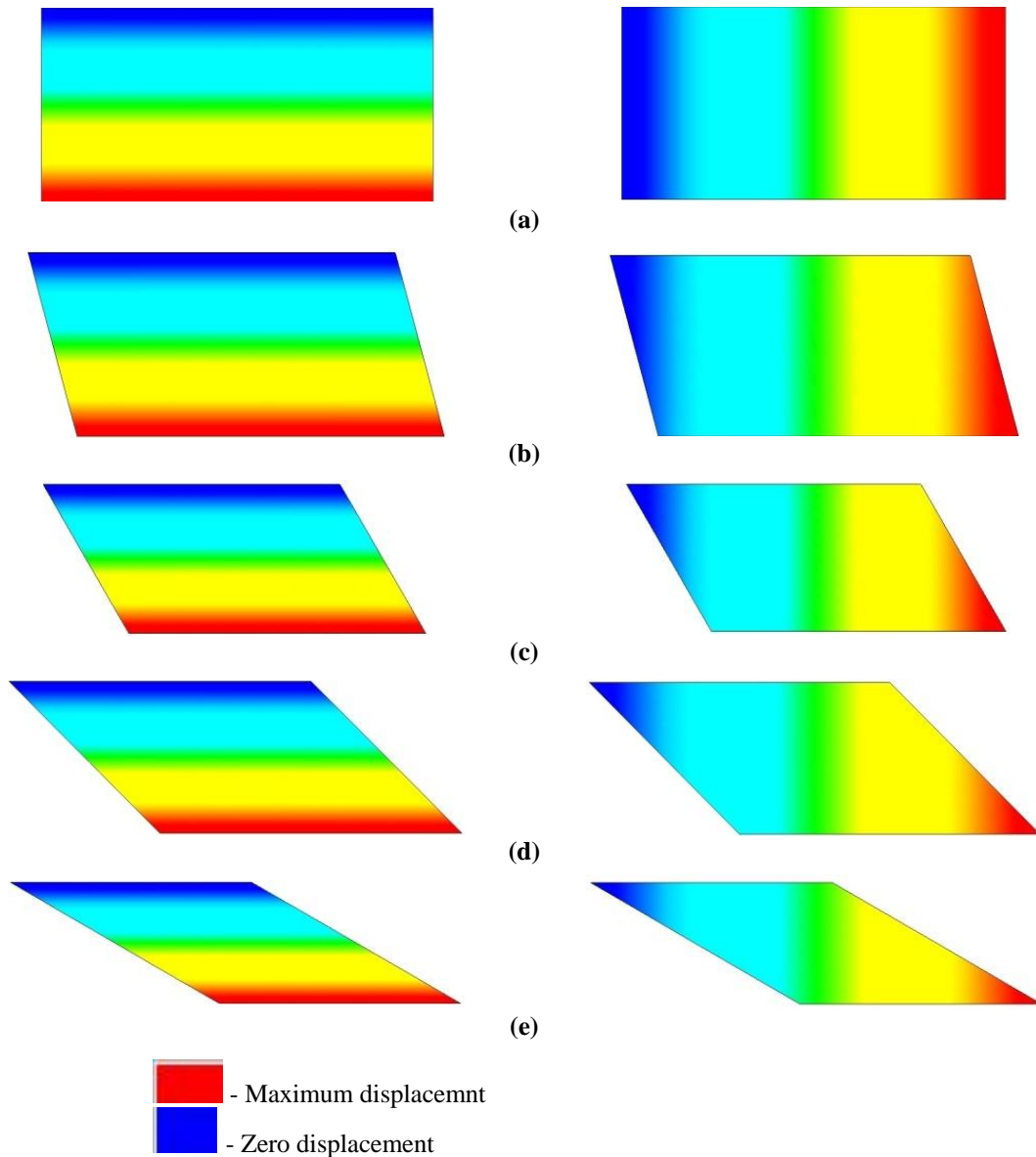


**Figure 2-31. Transverse (left) and longitudinal (right) displacement under the radial from center bearing condition for skew angles (a) 0° (b) 15° (c) 30° (d) 45° (e) 60°**

The simply supported straight bridge is not expected to develop any bending or torsion under thermal gradient loading. With increasing skew, combined bending and torsion develops under thermal gradient load. The longitudinal bending moment and torsion plots of simply supported bridges under negative temperature gradient are given in Figure 2-32 and Figure 2-33, respectively. Both bending and torsion is zero at both abutments and constant through the length of span. The bending moment increases with increasing skew angle. However, torsion increases with increasing skew up to 50°, but there is a sharp drop at the skew of 60°



(Figure 2-33). The reasons for this behavior need to be separately investigated with further refinement in skew angles and different span-to-width ratios.

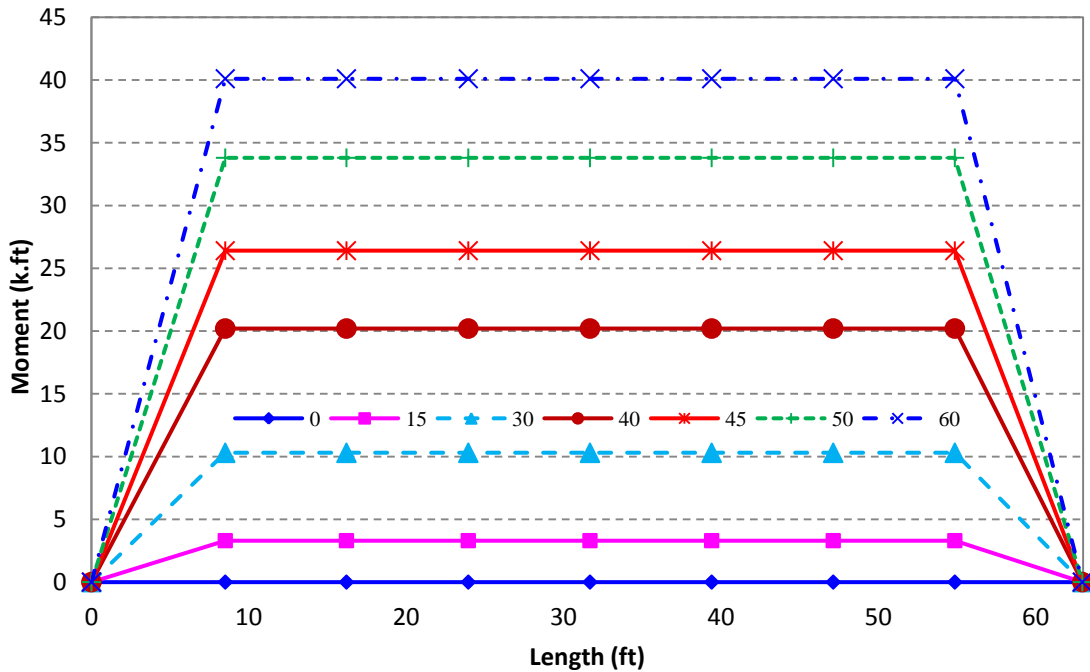


Figure 2-32. Longitudinal bending moment for full-width of simply supported stringer bridge under negative temperature gradient

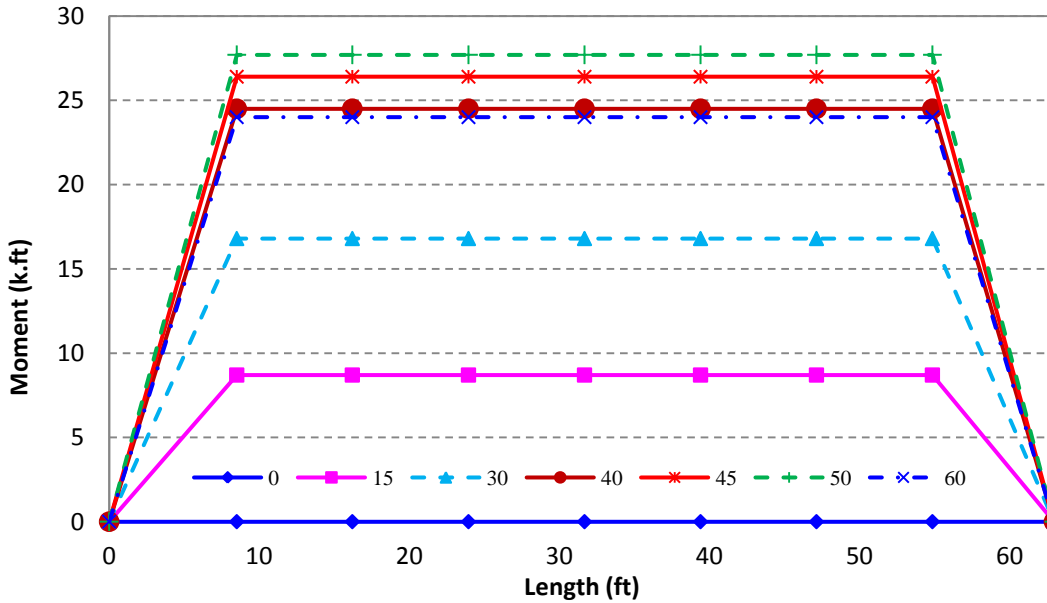


Figure 2-33. Torsion for full-width of simply supported stringer bridge under negative temperature gradient

## 2.4 DESIGN CHALLENGES OF SKEWED/JOINTLESS BRIDGES

### 2.4.1 Length, Skew and Curvature Limits

A typical maximum skew angle limit for jointless bridges specified by many states' highway agencies (SHAs) is 30° (Oesterle et al. 1999). However, maximum limit angle varies from 0° to no limit (Chandra et al. 1995). A 2004 survey (Maruri and Petro 2005) revealed that a majority of SHAs do not have restrictions on the maximum span length within the bridge, but they do limit the total length and the skew angle.

Table 2-1 summarizes the span length, total bridge length, skew, and curvature limits for prestressed concrete and steel girder bridges specified by the state highway agencies. The table was developed from the responses of 39 SHAs. For the purposes of this survey, Maruri and Petro (2005) specified bridge configurations as full integral abutment, semi-integral abutment, deck extension, and integral pier configurations.

**Table 2-1. Range of Design Criteria Used for Selection of Jointless Bridges  
(Maruri and Petro 2005)**

<b>Girder Type</b>	PC	Steel
<b>Maximum Span (ft)</b>		
Full Integral	60-200	65-300
Semi-integral	90-200	65-200
Deck extensions	90-200	80-200
Integral piers	120-200	100-300
<b>Maximum Total Bridge Length (ft)</b>		
Full Integral	150-1175	150-650
Semi-integral	90-3280	90-500
Deck extensions	200-750	200-450
Integral piers	300-400	150-1000
<b>Maximum Skew (Degrees)</b>		
Full Integral	15-70	15-70
Semi-integral	20-45	30-40
Deck extensions	20-45	20-45
Integral piers	15-80	15-No Limit
<b>Maximum Curvature (Degrees)</b>		
Full Integral	0-10	0-10
Semi-integral	0-10	0-10
Deck extensions	0-10	0-10
Integral piers	3-No Limit	0- No Limit

An additional point of reference outside the US is from the Ontario Ministry of Transportation. They limit the overall length of semi-integral bridges to 492 ft (150m) based on seasonal temperature variation considerations because of the capacity and efficiency of movement systems (Husain and Bagnariol 1999).

## 2.4.2 Volume Change Loads and Behavior of Jointless Bridges

Maruri and Petro (2005) used the survey data to identify the type of forces that states account for in the design of integral abutments such as earth pressure, temperature, creep, shrinkage, settlement, and additional forces due to skew or curvature (Figure 2-34).

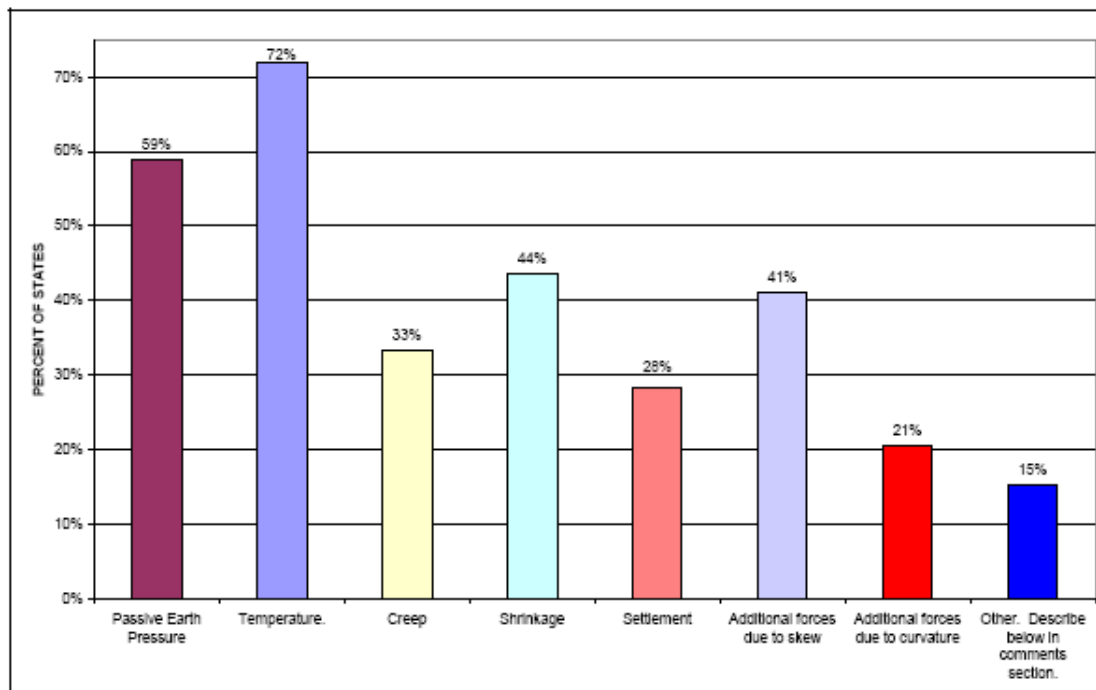


**Figure 2-34. Percent of states that account for different forces in the design of jointless bridges (Maruri and Petro 2005).**

Skew bridges respond to thermal loads with both longitudinal and transverse movements. Transverse movement magnitude depends on bridge geometry, level of restraints at the piers and abutments, skew or angle of crossing with respect to the abutments and/or piers, and magnitude of the thermal loads (Oesterle et al. 1999). Forces developed at the abutments due to thermal expansion are presented in Figure 2-35. According to Oesterle et al. (1999), transverse forces developed in the system are high enough to cause abutment and wing-wall

distress. For relatively short bridges, which undergo small expansions due to slight changes in effective temperature, the abutment needs to be designed to resist loads from batter piles and/or lateral passive soil resistance anticipating limited transverse deformations (Oesterle et al. 1999). Batter piles are inclined members that develop axial and shear forces due to abutment movement.

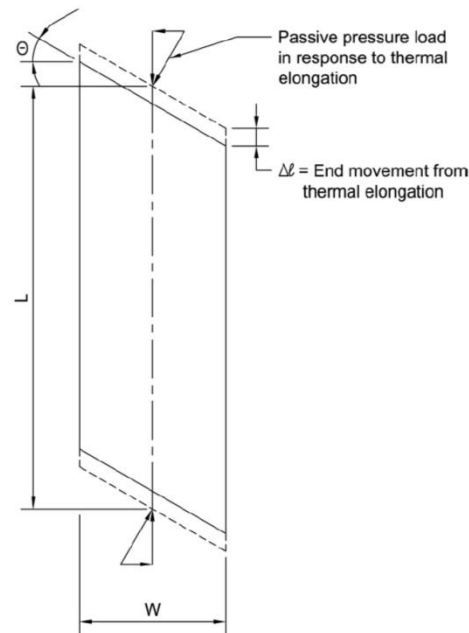


**Figure 2-35. Resultant force components that develop at the abutment under thermal expansion (Oesterle et al. 1999)**

According to Burke (1994a), skew in semi-integral bridges forces deck rotation about an axis normal to the plane of the deck. To resist the rotation, guide bearings and/or backwall guides are necessary. Guide bearings and/or backwall guides and a supporting structure need to be designed for the forces required to resist transverse movement.

The passive soil pressure forces behind the backwall due to superstructure elongation will not be collinear with the bridge axis and force deck to rotate (Burke 1994a, Figure 2-36). The rotation of semi-integral bridges and its effects have also been documented in the field (Sanford and Elgaaly 1993; Burke 1999; Van Lund and Brecto 1999). To prevent the deck rotation thus, to keep the superstructure of a skewed bridge stable, the force couple resisting rotation ( $P_p \tan \delta \times L \cos \theta$ ) must be equal or greater than the force couple causing rotation ( $P_p L \sin \theta$ ).

$$P_p \times L \sin \theta \leq (P_p \times \tan \delta \times L \cos \theta) \text{ (FS)} \quad (2-1)$$

Where

- $P_p$ : total passive pressure
- $\theta$ : skew angle
- $\delta$ : backfill-abutment interface friction angle
- $L$ : bridge deck length
- FS: factor of safety

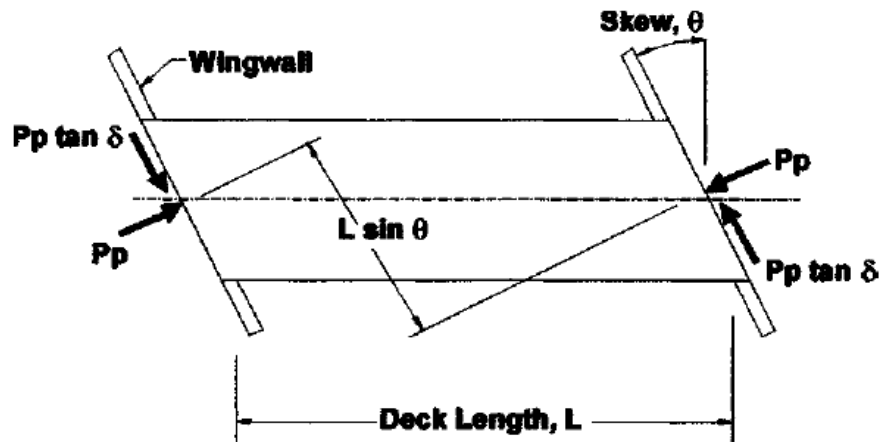


Figure 2-36. Forces on the bridge (Steinberg et al. 2004)

Providing a factor of safety of 1.5 and assuming an angle of friction of  $22^\circ$  at the structural backfill interface ( $\delta$ ), Burke (1994a) concluded that the bridge to remain stable, skew angle must be equal to or less than  $15^\circ$ . For greater skews, guide bearings and/or backwall guides can be provided to resist the forces generated by the restrained transverse movement. Based on this relationship, the required design strength of the guides needs to be equal to  $0.5 P_p$  for  $30^\circ$  skew, and  $0.7 P_p$  for  $45^\circ$  skew bridges.

Burke (1994a) also noted that the deck rotation motion may be reduced as a result of the approach slab-subbase friction, the shearing stiffness of the elastomeric bearings, and by the compressive stiffness of fillers in the movable joints between the superstructure and wingwalls.

Eq. 2-1 holds valid for single span bridges and multi-span bridges if the piers do not provide rotational resistance through the connection between the girders and piers. For bridges with integral piers or piers with fixed bearings, the unrestrained rotation of superstructures about a

vertical axis can induce torsion on the pier (Burke 1999). For example, consider the case of a  $40^\circ$  skewed two-span bridge with expansion bearings at both ends and fixed bearings at the pier. Under uniform thermal expansion, longitudinal reactions developing at the intermediate supports due to the nature of skew would tend to rotate the superstructure about its vertical axis. Since bearings at the abutment are not restrained for horizontal movement, the resisting twisting moment obtained can only develop at the piers. Thus, piers would experience significant twisting (Figure 2-37).

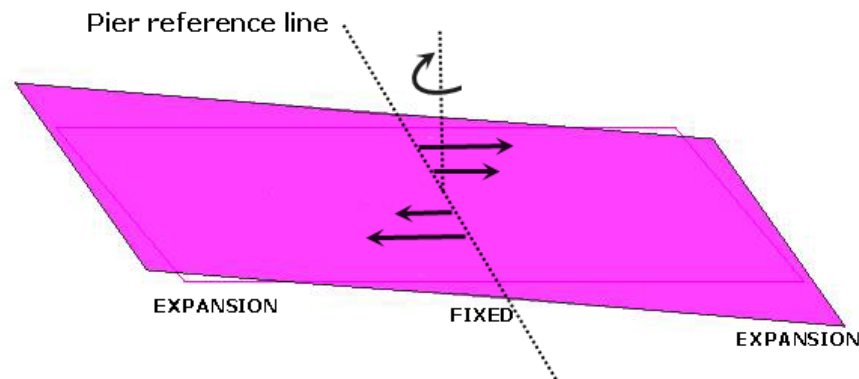


**Figure 2-37. Deformed shape of the deck of a two-span continuous skew stringer bridge under uniform expansion**

Steinberg et al. (2004) monitored the wingwall/diaphragm joint of two semi-integral bridges in Ohio. The first bridge had a single span of 87 ft, a roadway width of 32 ft and skew of  $65^\circ$ . The second bridge had four spans with a total length of 314 ft and a width of 40 ft at a skew of  $25^\circ$ . The maximum forces measured on the wingwalls were 35.7 and 30.1 kips, respectively. The finite element simulations revealed that lower skews would result in lower wingwall forces at lower backfill stiffness values. As the backfill stiffness increased, the wingwall reaction increased more rapidly at higher skews compared to lower skews.

Oesterle et al. (1999) stated that for bridges with skew greater than  $20^\circ$ , wingwalls should be designed for the forces that develop in the transverse direction. Further, U-shaped wingwalls are recommended for skewed bridges since they would help resisting transverse movement of the abutments.

### 2.4.3 Semi-Integral Abutment Details

Aktan et al. (2008) recommended changes to current MDOT semi-integral abutment details for straight and moderately skewed (up to 20° skew) bridges. MDOT current and proposed details are not presented here for brevity. Readers are encouraged to refer to Aktan et al. (2008) for details. Current effort is to document the best practices of a few selected SHAs to identify key details/configurations to improve the durability performance of high skew (20° < skew ≤ 45°) semi-integral and deck sliding over backwall bridge systems.

For skewed semi-integral and deck extension bridges, VDOT uses rub plates that act as a bearing between the superstructure and the wing haunch in the acute corners (Figure 2-38). The rub plates transfer horizontal force from the superstructure to the abutment, while allowing longitudinal sliding. Typically, rub plates are made of stainless steel with shear studs cast into concrete. This practice started after the rotation of integral bridges under passive pressure became evident during monitoring of a 5° skew, 323 ft long, and 85 ft wide bridge built in 1993. Rub plates have continuously been used since then regardless of size, skew and span configuration (Weakley 2005). This detail is amenable to the use of deck extensions with Massachusetts-type approach slab (Figure 2-39). Since the approach is buried below the plane of deck extension, there is no conflict with the superstructure longitudinal movement. There is potential for pavement damage due to deck expansion, if proper measures are not taken. However, there is no information related to the joint performance between the pavement and the extended deck.

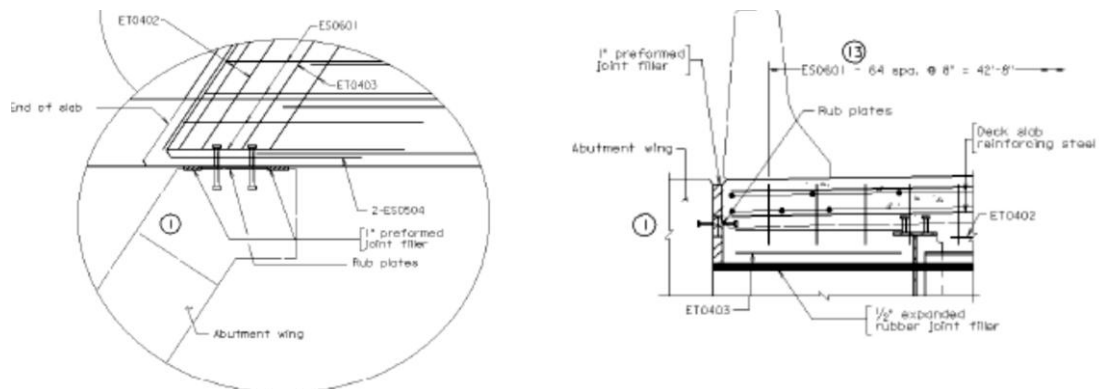
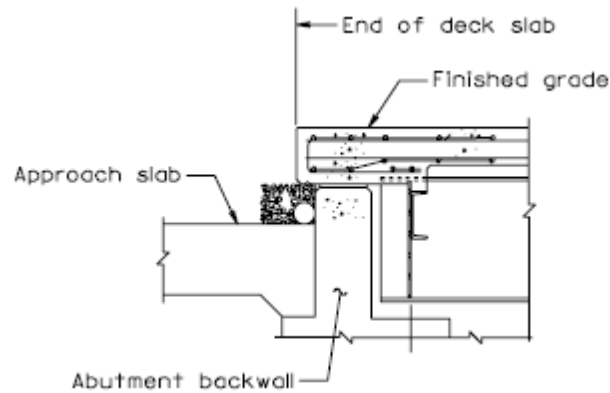


Figure 2-38. Rub plate detail (VDOT)



**Figure 2-39. VDOT deck extension detail with buried approach slab**

Burke (1994b) proposed a semi-integral abutment detail with an end diaphragm (a backwall) sliding with respect to a fixed abutment. With this concept, the restraint on the superstructure is reduced to passive pressure behind the backwall and resistance coming from bearings. This concept has some similarities to current MDOT (2006) practice but uses filler material for the vertical joints between the bridge deck and wingwalls. This detail requires end movement guides for both horizontal and vertical supports. The bearing for horizontal supports and the backwall need to be designed for passive pressure behind the backwall (Figure 2-40).



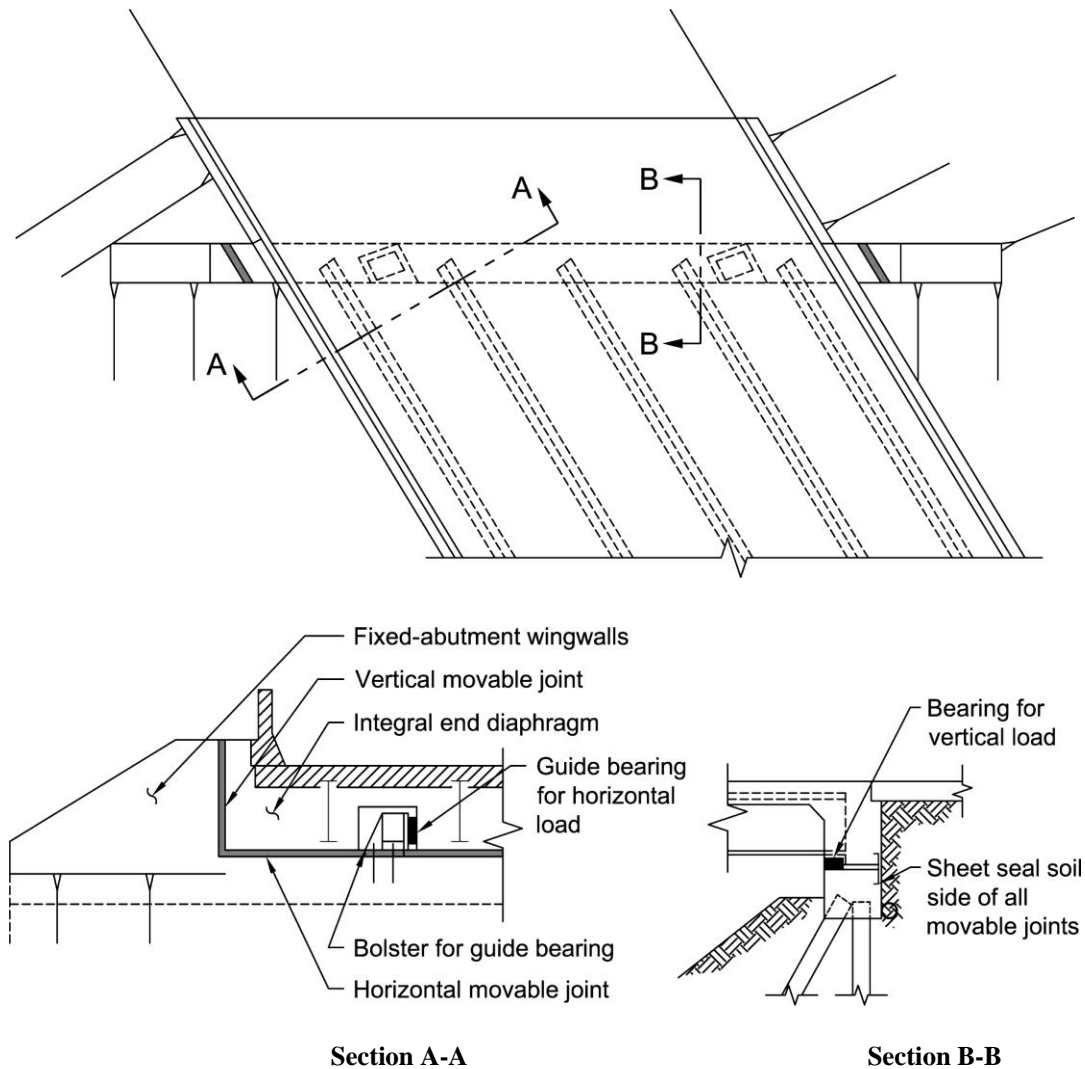


**Figure 2-40. Semi-integral abutment detail with end diaphragm moving over a fixed abutment  
(Burke 1994a and Oesterle et al. 1999)**

Ontario Ministry of Transportation does not impose skew limitations on semi-integral abutment bridges. However, skew bridges must comply with the following provisions (Husain and Bagnariol 1999):

1. *Lateral restraint should be provided to prevent superstructure rotation due to passive earth pressure.*
2. *The movement system at the end of the approach must be able to accommodate the deformations associated with the skew, and*
3. *The length of the wingwalls cantilevered from the abutment should be minimized.*

Figure 2-41 and Figure 2-42 show semi-integral abutment configurations for concrete girder bridges with overall span less than and greater than 328 ft (100 m), respectively. The major difference between these two configurations is the gap provided at the abutment-backwall interface (i.e., backwall configuration).

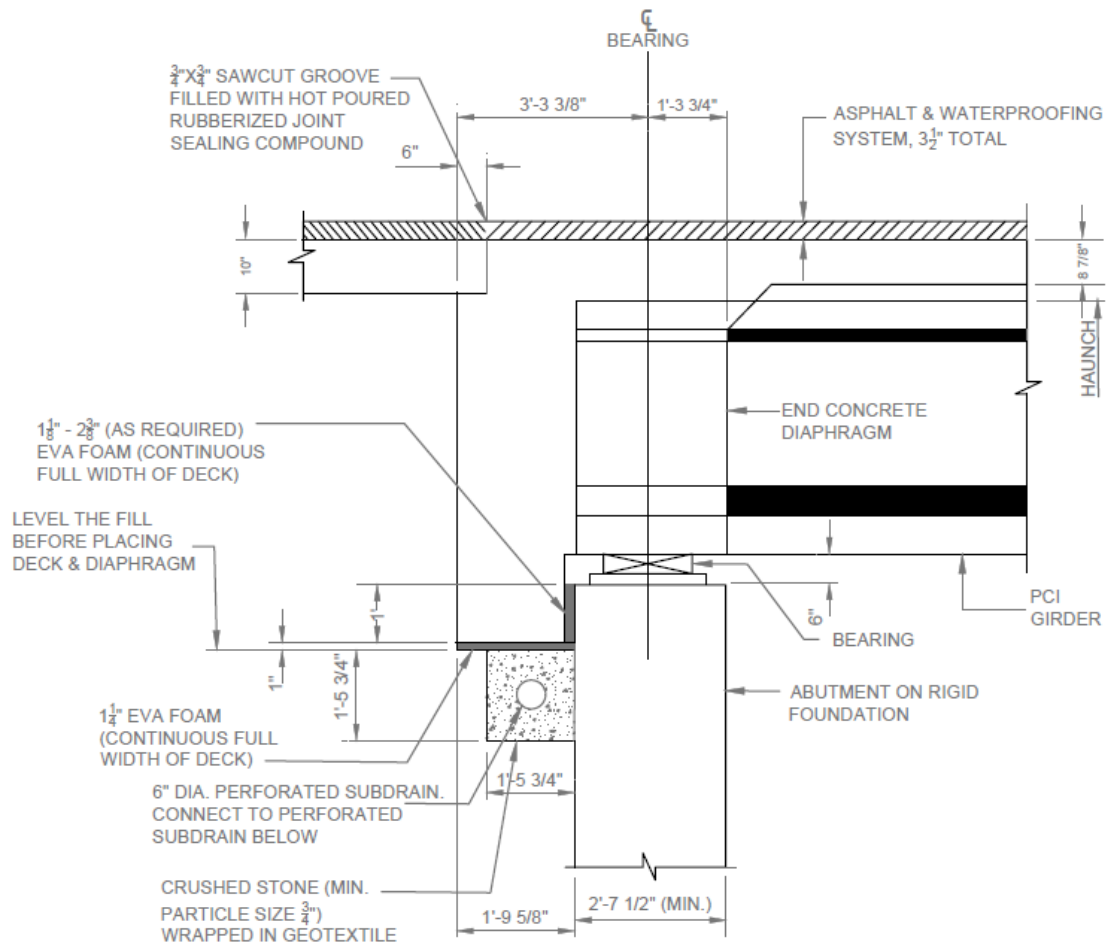


**Figure 2-41. Semi-integral abutment details of concrete girder bridge with overall span < 328 ft**

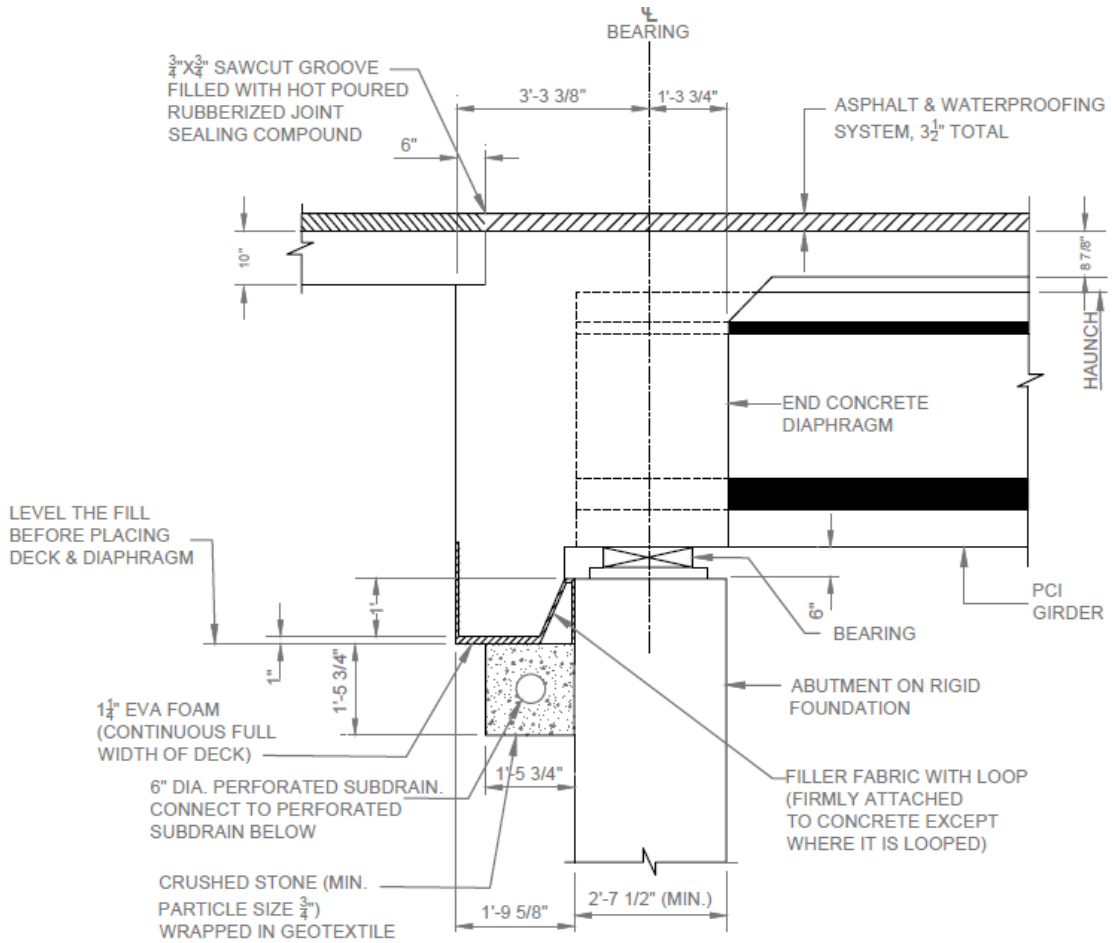


**Figure 2-42. Semi-integral abutment details of concrete girder bridge with overall span > 328 ft**

Figure 2-43 and Figure 2-44 show semi-integral abutment configurations for steel girder bridges with overall span less than and greater than 246 ft (75 m), respectively. The major difference between these two configurations is the gap provided at the abutment-backwall interface (i.e., backwall configuration).

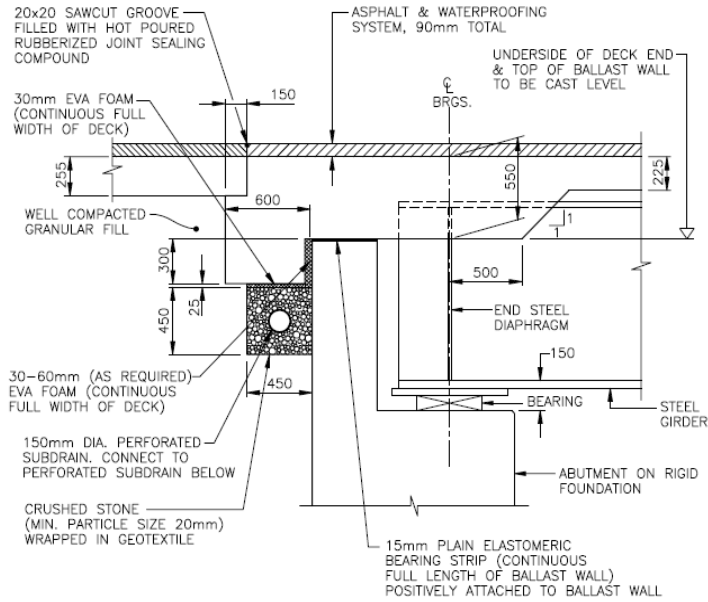


**Figure 2-43. Semi-integral abutment details of steel girder bridge with overall span < 328 ft**

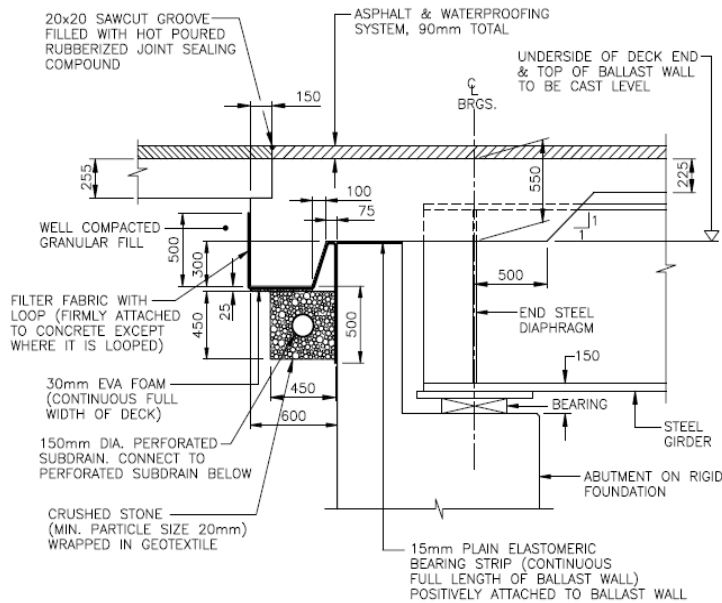


**Figure 2-44. Semi-integral abutment details of steel girder bridge with overall span > 328 ft**

Major aspects of Ontario details are: (1) allowing the deck to slide over the backwall when steel girders are used and (2) use of elastomeric bearing strips to provide a sliding surface between the backwall and the deck.

#### **2.4.4 EPS Backfill**

As discussed in the previous section, passive pressure developed by backfill generates a reactive force perpendicular to the backwall. In skew bridges, this force is not parallel to the longitudinal axis and, in the absence of adequate restraints, the force rotates the superstructure about an axis normal to the plane of the deck during bridge expansion. Providing restrains to prevent the rotation can induce large forces at the abutments or wingwalls. The high forces can cause cracking and other forms of distress if not properly accounted for in the design. In order to minimize the reactive force development due to backfill effects, expanded polystyrene (EPS) is being used by several states.

The Federal Highway Administration (FHWA) promotes the use of EPS geofoam as a backfill material for accelerated bridge construction projects. Several advantages of using EPS are rapid construction, reduced lateral load behind retaining structures, minimum differential settlement, etc (FHWA 2011).

The advantage of using EPS behind the backwall of integral or semi-integral systems is the attenuation of the effect of bridge movement on backfill during thermal expansion. Also, use of EPS behind the backwall is an effective means of reducing properly compacted backfill material settlement (Hoppe 2005). Figure 2-45 shows the abutment cross-section of experimental implementation of EPS by Virginia DOT (VDOT) in a semi-integral bridge.

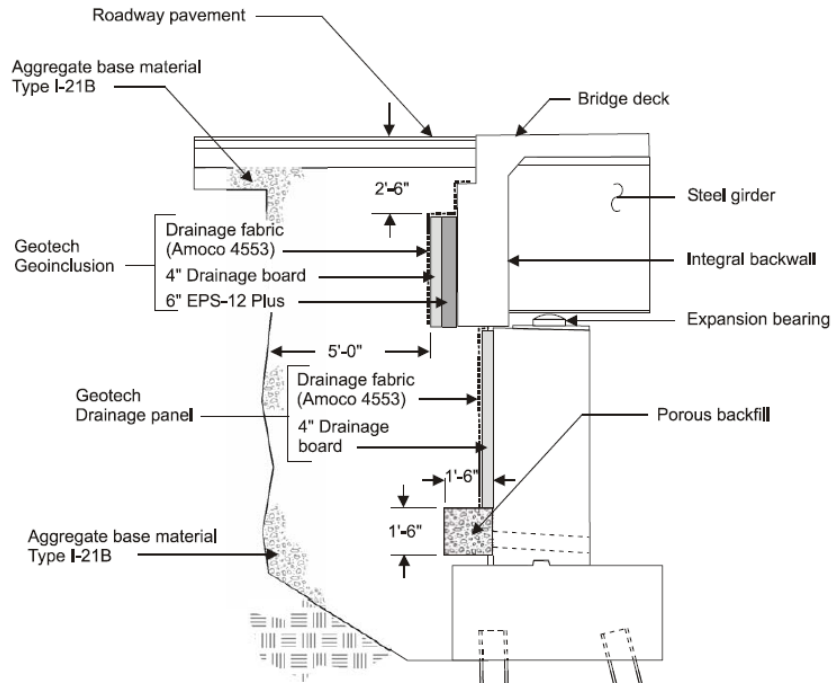


**Figure 2-45. VDOT semi-integral system with EPS (Hoppe 2005)**

The Structure and Bridge Manual of VDOT (2010) provides details on EPS implementation shown in Figure 2-45. Eq. 2-2 is recommended by VDOT for calculating the EPS thickness.

$$\text{EPS thickness (EPSt)} = 10 [0.01 h + 0.67 \Delta L] \geq 10 \text{ in.} \quad (2-2)$$

where,  $h$  is the height of the backwall in inches and  $\Delta L$  is the total bridge movement under the full temperature range. VDOT (2010) recommends using the passive earth pressure coefficient ( $K_p$ ) of 4 when EPS is used behind the backwall and analysis of the backwall considering a continuous beam supported by the girders. However, using field monitoring data of a  $45^\circ$  skew integral abutment bridge, Hoppe and Bagnall (2008) demonstrated that the  $K_p$  can be as low as 1.2 when the angle of backfill-abutment wall friction is  $20^\circ$  or 0.6 when the angle of friction is zero. Field observations have shown that the skew bridge superstructure rotation is as low as  $5^\circ$ ; hence, the interface angle of friction can be assumed to be zero (Hoppe and Bagnall 2008).

EPS properties such as compressive stress, elastic limit strain, modulus, Poisson's ratio, creep, durability, etc are discussed in the literature (Lutenegger and Ciufetti. 2009; Stark et al. 2004). EPS material properties are controlled by its density. For EPS with  $1.25 \text{ lb/ft}^3$

density, the elastic property limit is at a compression strain of less than 1%. The special provisions presented in Hoppe and Bagnall (2008) require providing EPS with linear-elastic stress-strain behavior up to 10 percent strain. In addition to density, EPS compressive strength is a nonlinear function of temperature. Strength remains constant for a temperature less than 32 °F. When the temperature increases beyond 32 °F and up to 73 °F, strength decreases at a rate of 7% per 18 °F. Conversely, temperature increase from 73 °F to 140 °F increases EPS strength at a rate of 7% per 18 °F.

For calculating the Poisson's ratio ( $\nu$ ) of EPS Lutenegeger and Ciufetti (2009) proposed the following equation:

$$\nu = 0.091\gamma + 0.0024 \quad (2-3)$$

where  $\gamma$  is the density of EPS in lb/ft<sup>3</sup>.

According to Lutenegeger and Ciufetti (2009), the coefficient of passive EPS pressure ( $K_p$ ) can be expressed in terms of Poisson's ratio as follows:

$$K_p = \nu / (1 + \nu) \quad (2-4)$$

For commonly available EPS, the passive earth pressure coefficient ( $K_p$ ) ranges from 0.1 to 0.2, negligible for design. Lutenegeger and Ciufetti (2009) state that the horizontal pressure, when a uniformly distributed load is applied over EPS, is about 1/10<sup>th</sup> of the vertical load. This shows that the magnitude of overburden pressure should be considered in analysis rather than using a constant value as recommended by VDOT. Creep of EPS is highly dependent on temperature. For example, at 140 °F exposure compared to 73 °F, uniaxial strains increased by 88% for 1.25 lb/ft<sup>3</sup> density EPS under a sustained stress of 626 lb/ft<sup>2</sup> for approximately 3 months. However, when the sustained stress is increased to 835 lb/ft<sup>2</sup>, with all other conditions remaining the same, creep strain increased to 195% (Lutenegeger and Ciufetti 2009).

Norway has a long history of using EPS, and significant data has been collected on EPS performance. According to Frydenlund and Aabøe (2001), EPS can be a very durable

material that can be used for a life cycle of 100 years provided that the buoyancy forces are properly accounted, EPS is well protected from dissolving agents like gasoline, and the stress level to which EPS is subjected is kept below 30-50% of its compressive strength.

Stark et al. (2004) illustrated some typical details of EPS abutment (Figure 2-46) where the approach is directly supported by a sand subgrade placed over the EPS. This detail is not preferable since the approach slab and the subgrade becomes a surcharge load over the EPS fill, which will promote EPS creep. This surcharge load can be eliminated by including a sleeper slab, to support the approach. From the design procedure presented by Stark et al. (2004), only active soil pressure will be the load acting on the abutment when the approach slab is supported by a sleeper slab. Passive earth pressure can be neglected as it can only form under large deformation within the EPS. Considering all the benefits, EPS is a practical solution to reduce the backfill effect on the backwall or abutment wall of skew bridges. When the use of EPS is specified, a sleeper slab should be provided to support the approach slab, buoyancy forces on the EPS should be accounted for in the design, and adequate protection should be provided using geotextile and gasoline containment geomembranes.

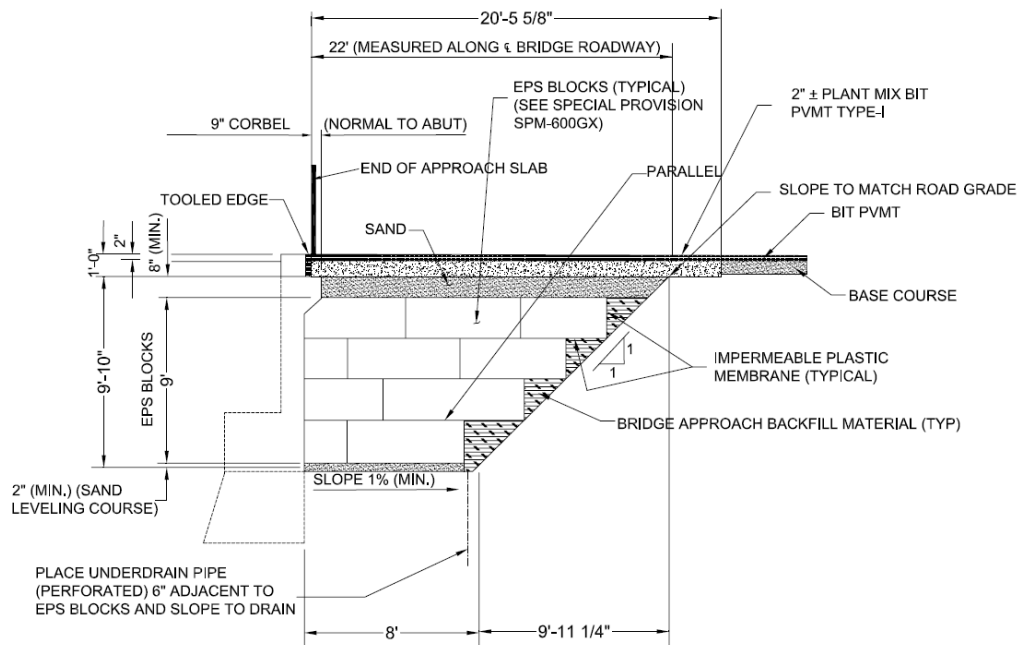


**Figure 2-46. Typical details of EPS abutment (Stark et al. 2004)**



### 2.4.5 EPS-Concrete Interface Friction

Several jointless abutment configurations are being used. One such configuration shown in Figure 2-47 is the deck sliding over backwall where a bond breaker is placed between the deck and the backwall. The function of the bond breaker is to provide a sliding surface between the deck and the abutment. When EPS is utilized as the bond breaker, there is a possibility to develop significant friction force on the sliding surface. According to Elragi (2011), the peak and residual friction coefficients between EPS and concrete are 2.3 and 1, respectively.

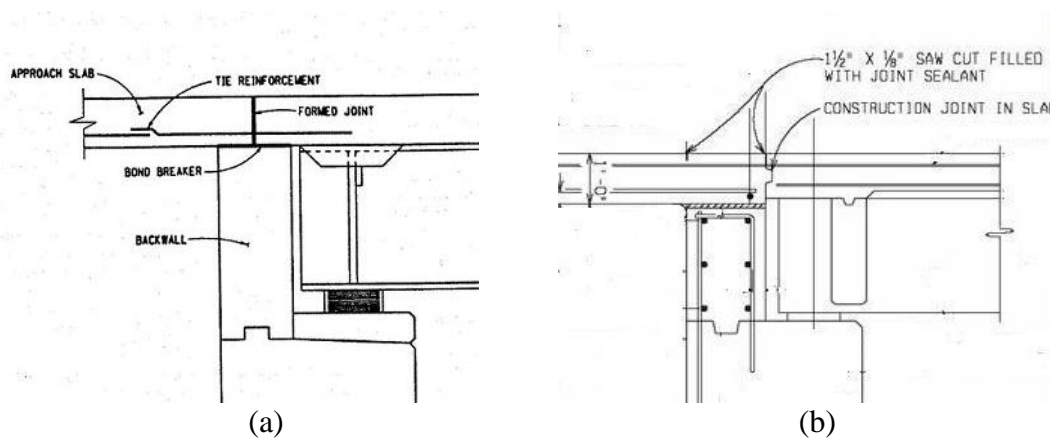


Figure 2-47. Deck sliding over backwall: (a) NYDOT and (b) MDOT

### 2.4.6 Support Bearing Selection and Design

Section 2.3 detailed literature recommendations on support bearing configurations to minimize stresses developed in the structure. As acknowledged in AASHTO LRFD (2010), a majority of these recommendations are not practical and cannot be implemented. Further, only a limited number of bearing types can be effectively used in semi-integral bridges (Table 2-2). Skew, semi-integral, or deck sliding over backwall bridges require bearings to allow longitudinal movement and rotation about all three axes and to provide resistance for transverse and vertical loads. Considering deformation and load demands on skew bridge support bearings, plain elastomeric pad (PEP), fiberglass-reinforced pad (FRP), and steel-reinforced elastomeric bearings or pads (SREB or SREP) are suitable for skew, semi-integral, or deck sliding over backwall bridges. Table 2-3 summarizes capabilities, limitations, and cost of bearings. Following load and translation magnitudes calculations, limitations given in the table can be used for preliminary selection (Roeder and Stanton 1996). Also, sliding

bearings can be combined with other types listed in Table 2-2 to accommodate large movements (Roeder and Stanton 1996; Parke and Hewson 2008).

**Table 2-2. Bearing Suitability (Source: AASHTO LRFD 2010)**

Type of Bearing	Movement		Rotation about Bridge Axis Indicated			Resistance to Loads		
	Long.	Trans.	Long.	Trans.	Vert.	Long.	Trans.	Vert.
Plain Elastomeric Pad	S	S	S	S	L	L	L	L
Fiberglass-Reinforced Pad	S	S	S	S	L	L	L	L
Steel-Reinforced Pad	S	S	S	S	L	L	L	S
Plane Sliding Bearing	S	S	U	U	S	R	R	S

*L: Suitable for limited applications; S: Suitable; R: May be suitable, but requires special considerations or additional elements such as sliders or guideways; U: Unsuitable.*

**Table 2-3. Summary of Bearing Capabilities (Source: Roeder and Stanton 1996)**

Type of Bearing	Load (kip)		Translation (in.)		Rotation (Rad.)	Cost	
	Min.	Max.	Min.	Max.	Limit	Initial	Maintenance
Plain Elastomeric Pads (PEP)	0	100	0	0.6	0.01	Low	Low
Fiberglass-Reinforced Pad (FRP)	0	135	0	1	0.015	Low	Low
Steel-Reinforced Elastomeric Bearing	50	785	0	4	0.04	Low	Low
Flat PTFE (Polytetrafluorethylene) Slider	0	> 2250	1	> 4	0	Low	Moderate

Roeder and Stanton (1996) and Badie, et al. (2001) developed charts for use in preliminary selection of bearings (Figure 2-48, Figure 2-49, Figure 2-50, and Figure 2-51). These charts were developed for steel girder bridges. But, they are equally valid for PC girder bridges. Other bearing types covered in the charts are pot bearing, cotton duck pads (CDP), and random oriented fiber pads (ROFP).

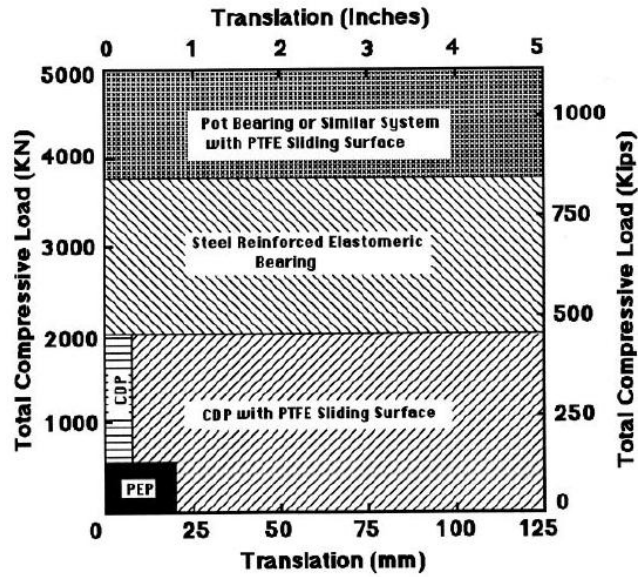


Figure 2-48. Preliminary bearing selection diagram for minimal design rotation (rotation  $\leq 0.005$  radians) (source: Roeder and Stanton 1996)

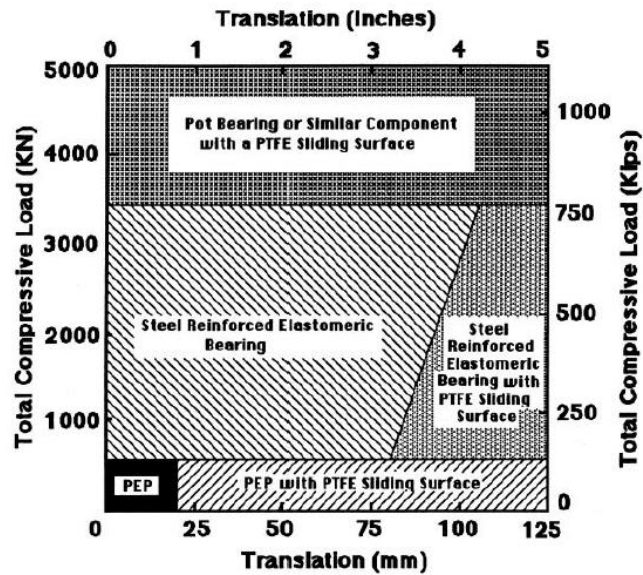


Figure 2-49. Preliminary bearing selection diagram for moderate design rotation (rotation  $\leq 0.015$  radians) (source: Roeder and Stanton 1996)

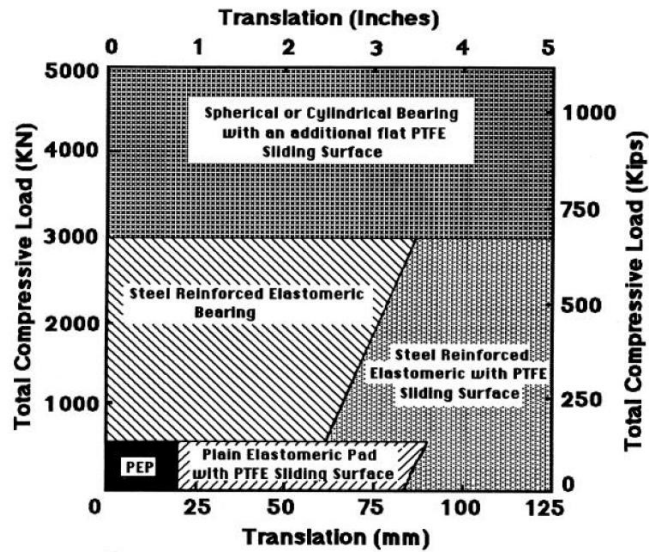


Figure 2-50. Preliminary bearing selection diagram for large design rotation (rotation > 0.015 radians) (source: Roeder and Stanton 1996)

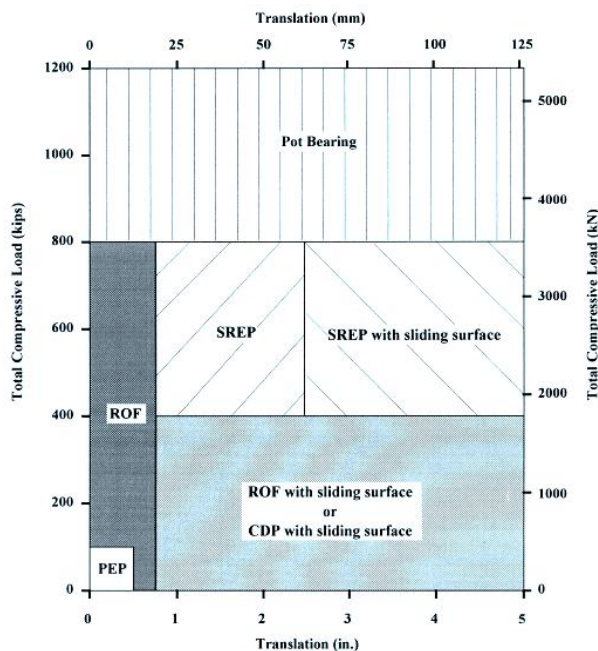
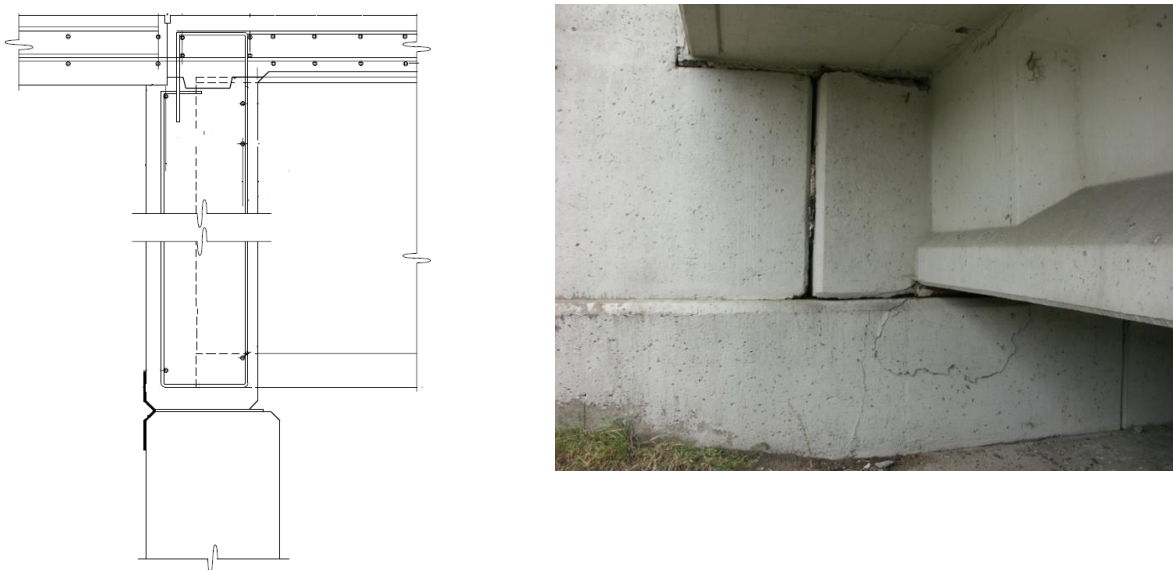


Figure 2-51. Preliminary bearing selection diagram (Badie, et al. 2001)

Inspection and maintenance are critical tasks in bridge management. Adequate access should be provided around the bearings for inspection, maintenance, and replacement (Parke and Hewson 2008; Roeder and Stanton 1996). In that regard, Ontario details (Figure 2-41, Figure 2-42, Figure 2-43, and Figure 2-44) are preferred over the current MDOT semi-integral details. In MDOT details, support bearings under the girders are encased by the backwall.

The joint filler between the backwall and the abutment establishes the sliding surface (Figure 2-52). In addition to concealing the support bearing, joint filler between the backwall and abutment used in this detail may generate large friction forces. High friction forces between the backwall and abutment may be the source of D-cracking documented on abutments of semi-integral bridges (Figure 2-52). The current design trend is to isolate the backwall from the abutment using configurations similar to Ontario and several other SHA. Implementation of these configurations allows the use of elastomeric bearings, sliding plate bearings or a combination thereof and minimizing interaction between the abutment and backwall. Further, isolation of the backwall from the abutment provides adequate space for inspection, maintenance, and replacement of bearings. However, isolation of the backwall from abutment requires developing specific design details to provide restraint to transverse movement of skew bridges. In that regard, placing the backwall over the abutment and restraining transverse movement by placing the wingwall against the backwall and deck, similar to current MDOT semi-integral details, provides many benefits if adequate measures are taken to minimize interface friction and infiltration of backfill material through the joints. One additional benefit of the current MDOT abutment-backwall configuration with different girder sizes is that restraint to lateral bridge movement is provided (Figure 2-53) equivalent to developing girder end restraint systems for skew bridges.



**Figure 2-52. MDOT semi-integral abutment configuration**



**Figure 2-53. Backwall and abutment configuration of a bridge with different girder depths**

### 2.4.7 Deck Reinforcement Details with Skew

According to Oesterle et al. (1999), reinforcement for skewed approach slabs should follow the skewed deck requirements of AASHTO LRFD (2010). The end of approach slab should be parallel to the abutment wall for both straight and skewed bridges.

AASHTO LRFD (2010) section 9.7.1.3 (Skewed Decks) for skew angle less than  $25^\circ$ , requires that the primary reinforcement to be placed in the direction of skew, otherwise placed normal to the girder axis (Figure 2-54). This provision is intended to prevent excessive deck cracking due to inadequate reinforcement in the direction of principal flexural stresses.

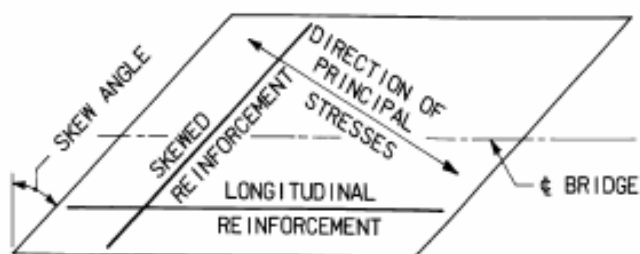


**Figure 2-54. Reinforcement layout (AASHTO LRFD 2007)**

According to section 9.7.2.5 (Reinforcement Requirements - Empirical Design) of AASHTO LRFD (2010), for a skew angle over  $25^\circ$ , the specified reinforcement in both directions shall be doubled in the end zones of the deck. Each end zone is the longitudinal distance equal to the effective length of the slab. This provision is also intended for crack control. It was documented that bridge decks with a skew greater than  $25^\circ$  have shown torsional cracks due to differential deflections in the end zone (OHBDC 1991). The extent of documented cracking was usually limited to a width equal to the effective length.

The MDOT Bridge Design Guide section 6.41.01 specifies bridge deck reinforcement layout when the deck is designed based on load factor method. “S along the skew” should be used to determine the slab reinforcement where S is the beam spacing minus the top flange width for slab on prestressed concrete I beams and beam spacing minus half flange width for slab on steel beams. If the angle of crossing is  $70^\circ$  or greater (i.e., skew is equal or less than  $30^\circ$ ), transverse bars are placed parallel to the reference lines if “S along the skew” falls in the same beam spacing range as “S normal to the beams” or the next larger range.

According to the MDOT Bridge Design Guide section 6.41.02 (Standard Bridge Slabs – Empirical Design), transverse bars may be placed parallel to the reference lines if the angle of crossing is  $65^\circ$  or greater (i.e., skew is equal or less than  $35^\circ$ ); they should otherwise be placed perpendicular to the bridge centerline. End zone reinforcement is required for both simply supported and continuous spans as shown in Figure 2-55.

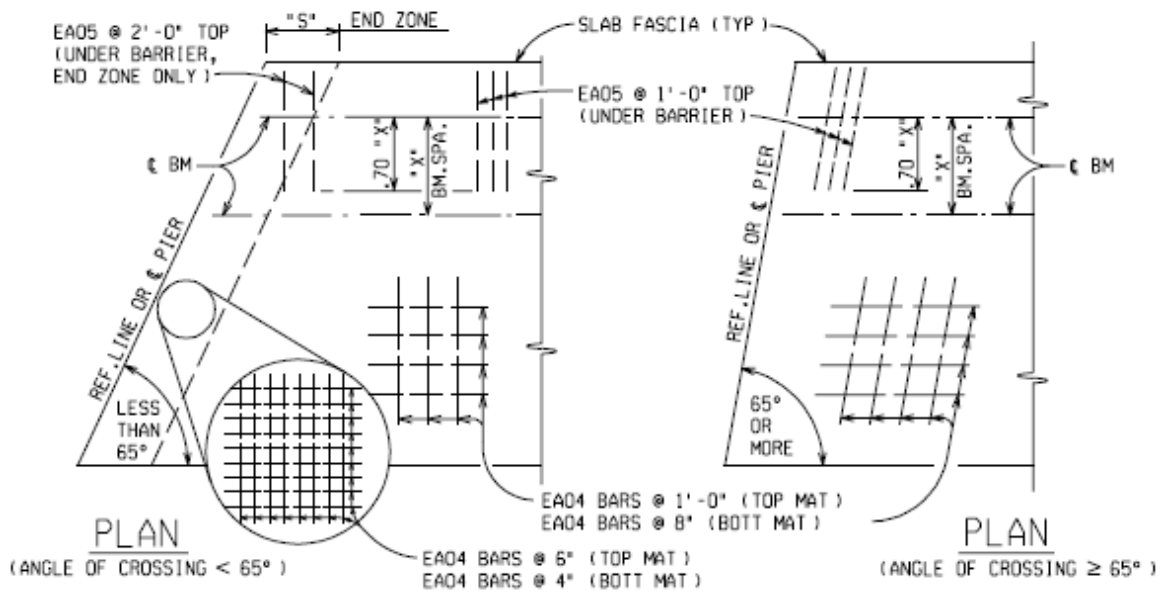


Figure 2-55. End zone reinforcement details (MDOT Bridge Design Guide 6.41.02)

## 2.5 FIELD PERFORMANCE OF SKEWED/JOINTLESS BRIDGES

The MDOT Structural Research Unit conducted field inspection of eight MDOT bridges that have link slab detail and were constructed between 2001 and 2003 (Gilani and Jansson 2004). Two of the bridges had moderate and high skew angles.

S08-63101 is a 26° skewed four-span steel bridge with a link slab over the center pier that was constructed in 2001 as part of a deck replacement project. Review of construction documents revealed that the longitudinal reinforcement was under-designed for HS-25 live loading. Inspection documented hairline cracks on the link slab within 1-2 feet of the saw cut region (Figure 2-56). Crack widths ranged between 0.002 and 0.004 inches. The rest of the link slab area was crack free.



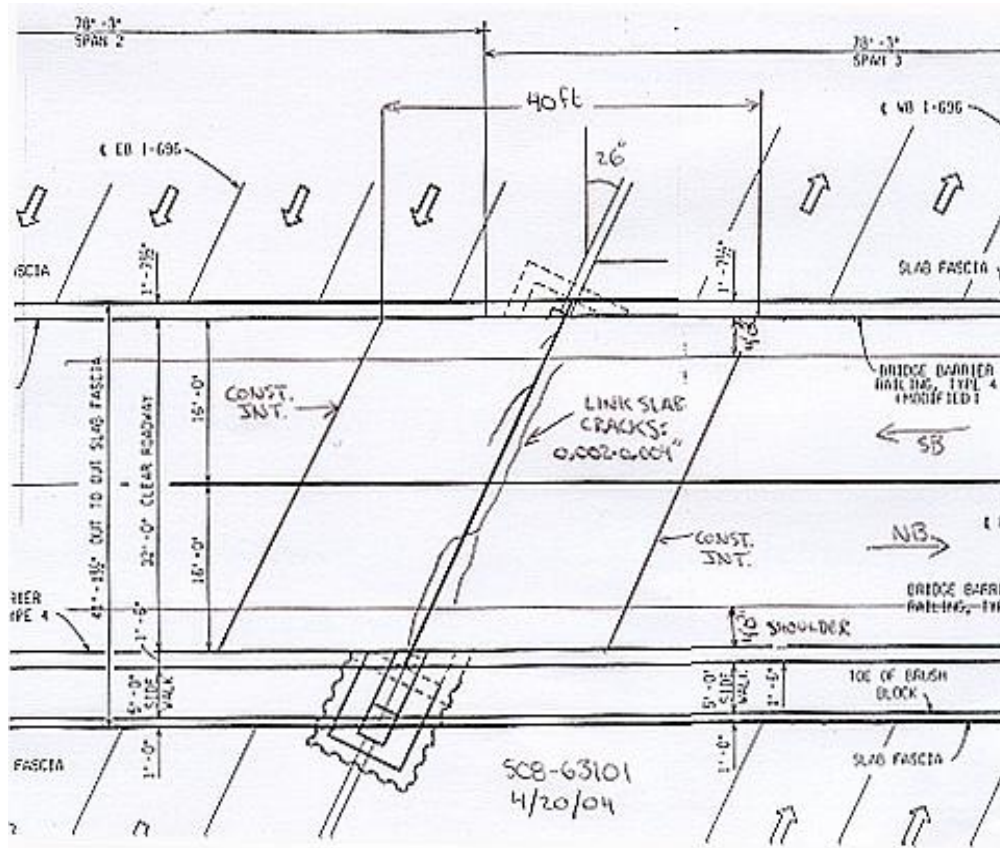
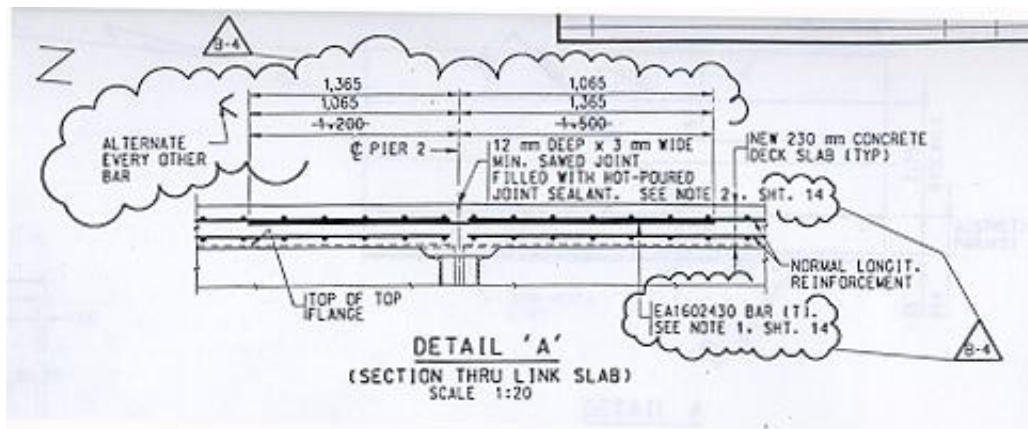


Figure 2-56. Link slab cracking on S08 of 63101 (Gilani and Jansson 2004)

S15-82025 is a four-span 45° skewed steel girder bridge. Link slab was constructed over the center pier in 2001 as part of a deck replacement project. Several pitfalls with design and construction were recorded: inadequate reinforcement, termination of the longitudinal reinforcement at the same location on both sides of the saw cut, unspecified pour sequence, and extra longitudinal reinforcement under the transverse reinforcement (Figure 2-57). The required area of longitudinal steel was calculated to be 1.40 in<sup>2</sup>/ft, and the quantity of as placed steel was 0.50 in<sup>2</sup>/ft. Despite the large difference in longitudinal steel between required and provided, the link slab in this structure appeared to be performing satisfactorily. ADT count on the bridge was only 600, with an ADTT count of zero. Despite the design and construction issues, typical link slab cracks were not documented during inspection (Gilani and Jansson 2004). It was believed that the light traffic with no truck loading might be the reason for the crack free link slab.



**Figure 2-57. Link slab design detail and an inspection photo (Gilani and Jansson 2004)**

North Carolina Department of Transportation (NCDOT) performed a follow up inspection to a high skew, 12-span bridge with link-slabs. The structure was opened to traffic for nearly two years. The link-slab saw cuts were filled with silicone. On the link slabs and the bridge deck only minor cracking parallel to the link slab was observed (NCDOT 2007).

The rotation of semi-integral bridges about its axis and its effects has been noted in the field (Sanford and Elgaaly 1993; Burke 1999; Van Lund and Brecto 1999). Indications of

significant transverse movement of abutments in bridges with high skews and/or horizontal curves were observed. Transverse movement of integral abutments should be accounted for in the design details for barrier walls, drainage structures, and the ends of the approach slabs (Tabatabai et al. 2005).

Figure 2-58 shows the abutment wall cracks near an acute corner of a two-span 45° skew bridge that sits on semi-integral abutments. The bridge was constructed in 1969 with an overall length of 292 ft and a width of 38 ft. The end-diaphragm moves with the superstructure that slides longitudinally, and it is guided transversely by relatively stiff abutments. Cracks in the abutment wall near the acute corner were perhaps caused by transverse forces (Nicholson et al. 1997 and Oesterle et al. 1999).

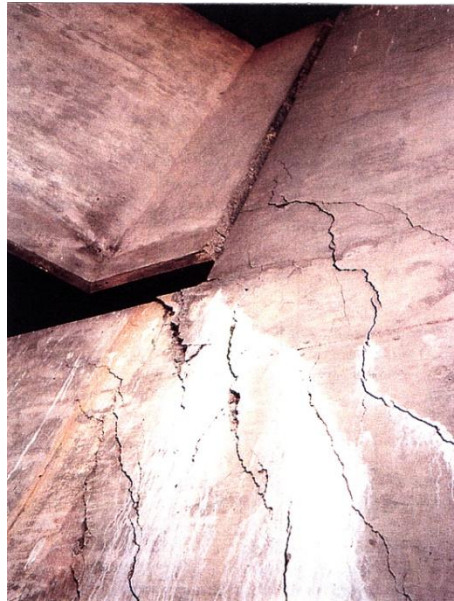


**Figure 2-58. Abutment wall cracking near an acute corner of the superstructure  
(Nicholson et al. 1997 and Oesterle et al. 1999)**

The Ontario Ministry of Transportation (OMOT) utilized various semi-integral abutment configurations since late 1960s. The most recent configuration, superseded by the details shown in Figure 2-41 to Figure 2-44, is shown in Figure 2-59. Use of this configuration was discontinued because the neoprene or rubber bearing pads placed in between the backwall and abutment wall did not prevent ingress of backfill material (Husain and Bagnariol 1999).



- reactions, and possibly uplift at acute corners. In general, negative moments are developed closed to obtuse corners; negative moments are a possibility at acute corners if uplift is prevented (Hambly 1991).
3. Skewed bridges with semi-integral abutments would tend to rotate about an axis normal to their horizontal plane. The rotation is due to the passive pressure developed behind the backwall under thermal expansion. Deck extensions also have a tendency to develop in-plane rotations but not as critical as semi-integral systems. In both deck extension and semi-integral systems, the rotation may be affected by the approach slab-subbase friction, the shearing resistance of the elastomers in the bearings, and by the compressive resistance of fillers used in the movable joints between the superstructure and wingwalls.
  4. The current MDOT deck sliding over backwall system uses EPS in between deck and backwall to introduce the sliding surface. The EPS elastic strain limit is very small and can deform beyond the elastic limit under deck self-weight and live loads. Further, peak and residual friction coefficients between EPS and concrete are 2.3 and 1.0, respectively. Because of these reasons, neoprene pads over the backwall may be used. In addition, a polyethylene sheet used under the approach should be extended to the backwall face on the span side to minimize friction at the interface.
  5. The current semi-integral configuration used by Ontario and several State Highway Agencies has the advantages of allowing the backwall to move independently from the abutment, providing access space for bearing inspection, maintenance, and replacement; and preventing backfill infiltration through the backwall.
  6. Isolation of the backwall from the abutment requires developing specific design details to constrain transverse movement of skew bridges. In that regard, placing the backwall over the abutment and restraining transverse movement by placing the wingwall against the backwall and deck, similar to current MDOT semi-integral details, provides many benefits if adequate measures are taken to minimize interface friction and infiltration of backfill material through the joints. Use of EPS from

- behind the backwall helps reduce passive earth pressure and prevents infiltration of backfill material.
7. One additional benefit of the current MDOT abutment-backwall configuration with different girder sizes is that restraint to lateral bridge movement is provided equivalent to developing girder end restraint systems for skew bridges. Adequate measures should be taken to minimize interface friction and infiltration of backfill material through the joints.
  8. Ontario uses EVA (Ethylene vinyl acetate, commonly known as expanded rubber or foam rubber) between the vertical faces of the backwall and abutment wall in order to allow the backwall to move independently from the abutment. EVA has a wider elastic range than EPS. On the other hand, the durability performance of EVA has not been documented.
  9. In order to allow the translation and rotation of skew bridges and provide sufficient load capacity, plain elastomeric pad (PEP), fiberglass-reinforced pad (FRP), and steel-reinforced elastomeric bearings or pads (SREB or SREP) are suitable for support bearings for semi-integral and deck sliding over backwall bridges. Also, PTFE sliding bearings can be combined with the support bearing types stated above to accommodate large superstructure movements. PTFE sliding bearings can be specified for most of the short and medium span bridges when girder end rotations are not critical.
  10. Rub plates, girder stops, or any other mechanism that is designed to resist large forces is needed to control lateral movement of skew bridges.
  11. With increasing backfill stiffness, forces at wingwalls of high skew bridges increase dramatically. EPS can be specified as a suitable backfill material for semi-integral bridges to reduce passive pressure. However, the approach slab should not be directly supported on EPS because of potential creep. EPS should also be protected using geotextiles and gasoline containment geomembranes.